Available online at www.sciencedirect.com

ScienceDirect

journal homepage: www.elsevier.com/locate/issn/15375110

Research Paper

Incorporating cultivar-specific stomatal traits into stomatal conductance models improves the estimation of evapotranspiration enhancing greenhouse climate management

Oliver Körner [a,*,1], Dimitrios Fanourakis [b,1], Michael Chung-Rung Hwang [c,d], Benita Hyldgaard [e], Georgios Tsaniklidis [f], Nikolaos Nikoloudakis [g], Dorthe Horn Larsen [c,h], Carl-Otto Ottosen [e], Eva Rosenqvist [c]

[a] Leibniz-Institute of Vegetable and Ornamental Crops (IGZ), Großbeeren, Germany
[b] Laboratory of Quality and Safety of Agricultural Products, Landscape and Environment, Department of Agriculture, School of Agricultural Sciences, Hellenic Mediterranean University, Estavromenos, 71004, Heraklion, Greece
[c] Department of Plant and Environmental Sciences, University of Copenhagen, Hoejbakkegaard Alle 9, 2630 Taastrup, Denmark
[d] Klasmann-Deilmann Asia Pacific Pte. Ltd, Singapore
[e] Department of Food Science, Aarhus University, Agrofoodpark 48, 8200 Aarhus N, Denmark
[f] Institute of Olive Tree, Subtropical Plants and Viticulture, Hellenic Agricultural Organization 'Demeter' (NAGREF), P.O. Box 2228, 71003 Heraklio, Greece
[g] Cyprus University of Technology, Department of Agricultural Sciences, Biotechnology and Food Science, Cyprus
[h] Horticulture and Product Physiology Group, Wageningen University, Wageningen, the Netherlands

ARTICLE INFO

Article history:
Received 22 October 2020
Received in revised form
27 March 2021
Accepted 17 May 2021
Published online 9 June 2021

Keywords:
Climate control
Relative air humidity
Simulation model
Stomatal conductance
Stomatal density
Transpiration

The effect of considering cultivar differences in stomatal conductance (g_s) on relative air humidity (RH)-related energy demand was addressed. We conducted six experiments in order to study the variation in evapotranspiration (ET_c) of six pot rose cultivars, investigate the underlying processes and parameterise a g_s-based ET_c model. Several levels of crop ET_c were realised by adjusting the growth environment. The commonly applied Ball–Woodrow–Berry g_s-sub-model (BWB-model) in ET_c models was validated under greenhouse conditions, and showed a close agreement between simulated and measured ET_c. The validated model was incorporated into a greenhouse simulator. A scenario simulation study showed that selecting low-g_s cultivars reduces energy demand (≤5.75%), depending on the RH set point. However, the BWB-model showed poor prediction quality at RH lower than 60% and a good fit at higher RH. Therefore, an attempt was made to improve model prediction: the *in situ*-obtained data were employed to adapt and extend either the BWB-model, or the Liu-extension with substrate water potential (Ψ; BWB-Liu-model). Both models were extended with stomatal density (D_s) or pore area. Although the modified BWB-Liu-model (considering D_s) allowed higher accuracy ($R^2 = 0.59$), as compared to the basic version ($R^2 = 0.31$),

* *Corresponding author.*
E-mail address: koerner@igzev.de (O. Körner).
[1] Equal contribution to this study.

https://doi.org/10.1016/j.biosystemseng.2021.05.010

the typical lack of Ψ prediction in greenhouse models may be problematic for implementation into real-time climate control. The current study lays the basis for the development of cultivar specific cultivation strategies as well as improving the g_s sub-model for dynamic climate conditions under low RH using model-based control systems.

Nomenclature

α_l	leaf photochemical efficiency ([mol CO_2] [mol photons]$^{-1}$)
a	empirical parameter modified BWB-Liu model (–)
A_s	individual stomatal area (μm^2)
A_p	pore area (μm^2)
B	Ball index (mol m^{-2} s^{-1})
β	empirical parameter Van Genuchten (–)
BWB-model	Ball-Woodrow-Berry model
BWB-Liu-model	BWB-model modified by Liu
c	measuring errors' correction (–)
C_s	air CO_2 partial pressure at the leaf surface (μbar)
D_s	stomatal density (number mm^{-2})
DSS	decision support system
ET_c	crop evapotranspiration (L plant^{-1})
g_s	stomatal conductance (mol m^{-2} s^{-1})
$g_{s,meas}$	measured g_s (mol m^{-2} s^{-1})
$g_{s,sim}$	modelled g_s (mol m^{-2} s^{-1})
g_0	minimum (residual) g_s as P_{nl} reaches 0 (mol m^{-2} s^{-1})
h_s	leaf surface RH fraction (–)
I	short-wave radiation (W m^{-2})
λE	latent heat of evaporation (J m^{-2} s^{-1})
m_s	adjustment factor (–)
m_g	empirical parameter Van Genuchten (–)
n_g	empirical parameter Van Genuchten (–)
n	empirical parameter BWB-Liu model (–)
Q_h	heat energy consumption (MJ m^{-2})
p_a	Atmospheric pressure (kPa)
P_{nl}	leaf net photosynthesis rate (μmol m^{-2} s^{-1})
$P_{nl,max}$	maximum leaf net photosynthesis (μmol m^{-2} s^{-1})
PPFD	photosynthetic photon flux density (μmol m^{-2} s^{-1})
Ψ	substrate water potential (kPa)
RH	relative air humidity (%)
SLA	specific leaf area (cm^2 g^{-1})
θ	volumetric water content (v v^{-1})
θ/θ_s	effective water content (v v^{-1})
θ_r	residual water content (v v^{-1})
θ_s	saturated water content (v v^{-1})
VPD	vapour pressure deficit (kPa)
w_{pd}	dry pot mass (g)
w_{pf}	fresh pot mass (g)
z	canopy levels

1. Introduction

Climate-controlled greenhouses are high energy-consuming facilities, especially in hot or cold regions (Bot, 2001; Vanthoor, 2011, p. 307). Since the early 1990's, energy demand has been reduced by the introduction of crop directed climate control regimes with dynamic temperature boundaries (e.g. Aaslyng et al., 2003; Körner & Challa, 2003a). These exploit the naturally-occurring diurnal temperature fluctuations without the need for heating to a fixed temperature, achieving up to 18% savings in energy use for heating in e.g. Dutch climate conditions (Körner et al., 2004). Increasing greenhouse insulation (i.e., semi-closed and closed greenhouse systems) has further reduced energy use required for heating (Gelder et al., 2012; Opdam et al., 2005). However, temperature and relative air humidity (RH) control remain the two main challenges in these concepts (Körner & Challa, 2003b; Vadiee & Martin, 2012). Potential risks with accidental rise of RH above 85% include increased incidence of fungal diseases (e.g., powdery mildew and botrytis; Mortensen et al., 2007), induction of physiological disorders such as the blossom-end rot in fruit vegetables (Fanourakis, Aliniaeifard, et al., 2020; Ho et al., 1993) and, in the long-term, the development of stomata with reduced closing ability (Fanourakis, Bouranis, et al., 2016; Giday et al., 2014). Although the occurrence of malfunctional stomata remains undetected during cultivation, it becomes apparent when plants rapidly wilt upon exposure to lower RH such as during display (Carvalho et al., 2016; Fanourakis et al., 2015, 2019a). However, the objective of keeping RH below 85% is counteracting the striving for low energy demand. The energy needed for dehumidification (by heating) increases when RH is adjusted to lower levels. Despite great efforts devoted to the development of more efficient dehumidification methods, reducing RH to a secure level (≤85%) remains rather costly, accounting for about 20% of annual energy demand in Northern European climates (Körner & Van Straten, 2008). As such, improved RH control will lead to a major decrease in both energy demand and CO_2 footprint, combined with a better (visual and inner) quality of the produce. In vegetable crops, inner quality refers to the nutritional value (Amitrano et al., 2021; Zhang et al., 2017), whereas in ornamental crops to the keeping quality (Carvalho et al., 2016; Fanourakis et al., 2016b, 2020b). Since the crop itself is a major driver of RH via crop evapotranspiration (ET_c), its accurate estimation is essential for greenhouse climate control.

The ET_c depends on both environmental conditions [e.g. short-wave radiation, vapour pressure deficit (VPD) and air flow] and crop-related factors [e.g. crop/plant architecture and leaf stomatal conductance (g_s)]. Despite its obvious importance, models estimating ET_c mostly ignore some or all of

these crop-specific factors, based on the lack of relevant parameters for the wide variety of crops and cultivars. Most investigators dealing with g_s estimations use the concept of Ball–Woodrow–Berry (BWB) (Ball et al., 1987). The BWB concept describes the relationship between g_s and net photosynthetic rate (P_n) using two factors, i.e. minimal stomatal conductance (g_0) and an empirical sensitivity coefficient for the slope (m_s). In that, the inputs to the combined $P_n - g_s$ model are commonly measured climate or microclimate variables: short-wave radiation (I, W m^{-2}), CO_2 (μmol mol^{-1}), temperature (°C) and RH (%). Although the model is widely used, it has been found to underestimate g_s and transpiration in roses (Kim & Lieth, 2003) and to be less suitable at conditions with high temperature and elevated CO_2 (Janka et al., 2016). To improve the BWB model, soil water potential (Ψ) as additional variable has been introduced adjusting the value of m_s (Liu et al., 2009). The resultant BWB-Liu-model has shown improved accuracy of g_s estimation under different irrigation regimes (Liu et al., 2009). However, two issues remain: 1) through the global parameterisation of the BWB type models applied to a wide range of crops and varieties, the crop and cultivar specific parameters induce a mismatch between model predictions and reality; 2) the newly introduced parameter Ψ in the BWB-Liu-model is difficult to access in common greenhouses and climate control regimes, as it needs additional measurements of the root zone, while the remaining input variables of the BWB-model are commonly available climate variables in both greenhouses and simulators.

Despite the rather limited usability of the simple BWB-model in commercial practise under dynamic climate conditions (e.g., high temperatures, elevated CO_2, and highly fluctuating RH) and uncertain parameterisation, its practical advantage of not needing measured Ψ as input could in some situations cover for the misfit. In this paper, we address the pros and cons of both models and present a possible improvement to them. We focus on the variability of ET_c and g_s in selected rose cultivars with similar external appearance, aiming to show the effect of cultivar specific BWB-model parameters on prediction quality and effect in model application to predictive greenhouse climate control.

We hypothesise that there are further possibilities for improvements to the BWB-model types by including cultivar specific traits into the model, i.e. the stomatal pore area (A_p) and stomatal density (i.e. stomatal number per unit area; D_s). These factors vary considerably not only between taxa, but also among cultivars of a given species (Giday et al., 2014). A_p is dynamically adjusted by changes in pore aperture, since pore length is rather rigid during opening and closure of stomata (Fanourakis et al., 2014; Franks et al., 2009; Islam et al., 2019). Active pore aperture adjustments in response to internal (e.g. water status) and external (environmental) factors are physiologically regulated (Fanourakis et al., 2013). Instead, pore length and D_s are anatomical features, which are set during leaf elongation (Dow et al., 2014; Fanourakis et al., 2014). Therefore, by integrating A_p or D_s, as factors determining operating g_s, the ET_c estimation is expected to improve.

The current study presents the importance of cultivar specific parameterisation of a g_s-model for application in predictive greenhouse climate control in a simulation study with an existing greenhouse simulator (Goddek & Körner, 2019; Körner & Hansen, 2012; Körner & Holst, 2017). To test the hypothesis that employing low-transpiring genotypes will improve energy saving (required for dehumidification), a comparative simulation study of energy demand at different climate setpoints with two cultivars was performed. Given that this hypothesis is validated, it is possible that 1) measures of g_s may add value in selection indices of pot plant breeding programs, since these directly affect the energy demand which is related to RH control, and 2) parameterising the BWB-model types for each crop and cultivar in a monoculture enables energy saving options for model-based greenhouse climate controllers. Rose was employed as the model system since it is one of the most important ornamental crops, and a species in which genetic differences in terms of ET_c have been observed.

2. Materials and methods

The current paper analyses the effect of genetic differences in stomatal conductance (a major driver for ET_c) on greenhouse humidity-related energy demand. The effect of climate variables is researched, and possible solutions for a combined strategy on genetic breeding and model-based climate control are suggested. In that, a step-by-step approach was employed, including physiological investigations, model development, calibration and validation, model selection and implementation, and eventually a simulation study (Fig. 1).

2.1. Experimental set-up

2.1.1. Plant material

In all six experiments, pot roses (*Rosa x hybrida*) with four cuttings per 0.55 L pots grown in a mixture of peat and perlite (9:1, v/v) (Mega Substrates BV, Rotterdam, The Netherlands) were obtained from a commercial grower (Rosa Danica, Marslev, Denmark). Before transfer to the respective experimental units, plants were pruned (second cut) leaving two nodes on the main shoot, each bearing a leaf and its axillary bud. The plants were well-watered upon arrival, and mean pot mass was assessed following drainage (330 g). Six experiments were conducted in total (summarised in Table 1). Experiments (Exp.) 1–3 were arranged in walk-in growth chambers (Aarhus University, Aarslev, Denmark), while the other three (4–6) were carried out in greenhouse compartments (University of Copenhagen, Taastrup, Denmark). In growth chamber experiments the effect of one specific environmental variable on ET_c was tested against stable conditions, whereas in greenhouse experiments this was performed under fluctuating conditions. Depending on the experiment, different environmental factors expected to induce variation in ET_c were manipulated (Table 1).

2.1.2. Climate chamber setup and growth conditions (Exp. 1–3)

The walk-in climate chambers (MB Teknik, Brøndby, Denmark) were fitted with high-pressure quartz lamps (HQI-BT 400W/D Pro, Slovakia) providing a photosynthetic photon flux density (PPFD) of 300 μmol m^{-2} s^{-1} determined by a quantum sensor (LI-250A, LI-COR, Lincoln, NE, USA) with 18 h photoperiod. The CO_2 concentration was controlled by a flux

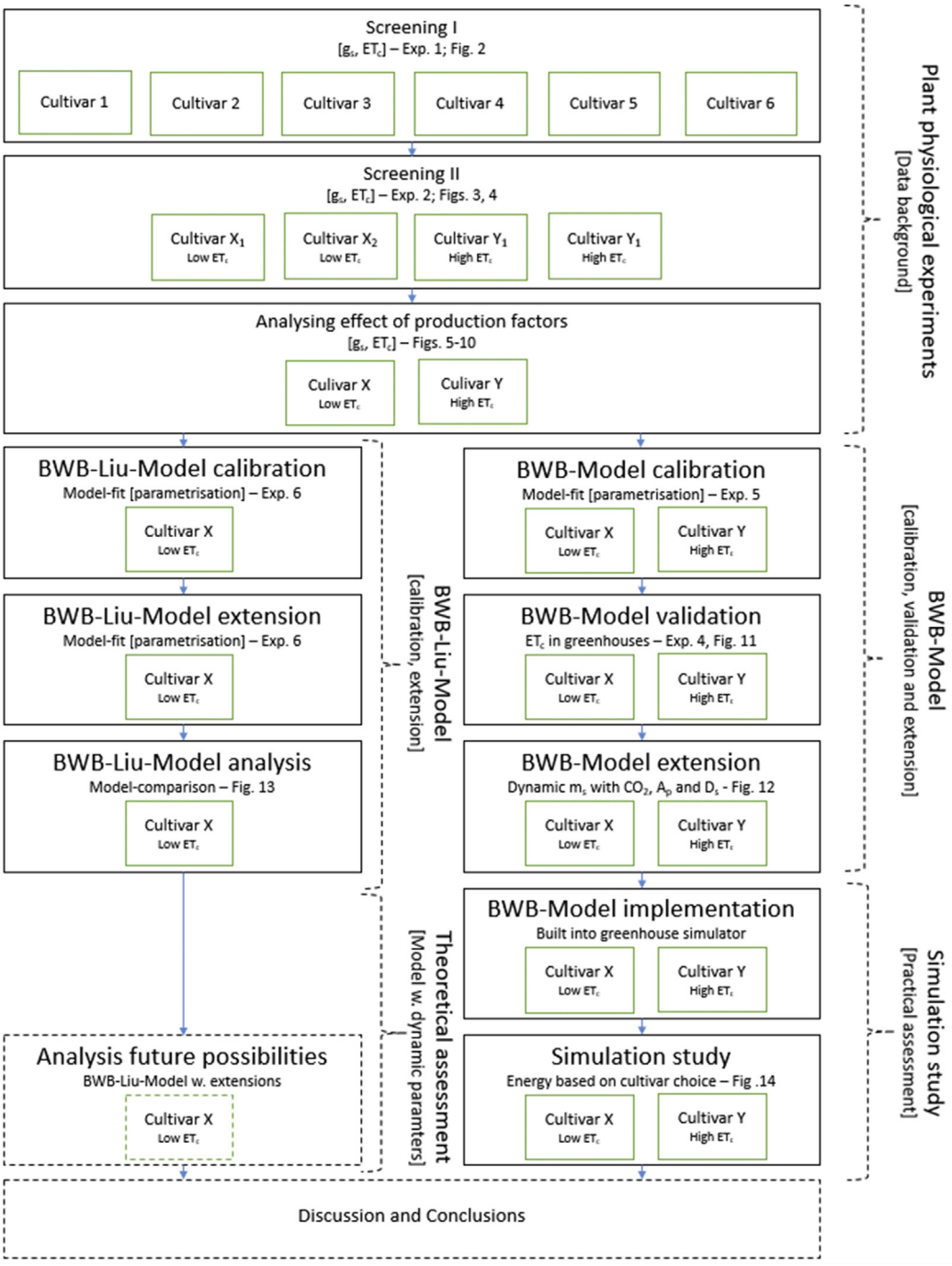

Fig. 1 – Structure of the assessment strategy including figures as used in this paper. With Ball-Woodrow-Berry-Model (BWB); With Ball-Woodrow-Berry-Liu-Model (BWB-Liu), crop evapotranspiration ET_C, stomatal conductance (g_s), stomatal pore aperture (A_p), stomatal density (D_s), model parameter constant (m_s).

controller and infrared gas-analyser (EGM-3, PP Systems, Amesbury, MA, USA) and set to 400 μmol mol^{-1}. The irrigation regimes were controlled by two Drought Spotter units (±0.1 g; Phenospex, Heerlen, The Netherlands), each containing 24 single-pot balances. A full nutrient solution was used with pH of 5.5 and EC of 2.0 mS cm^{-1} (Fanourakis et al., 2008). In addition to the climate sensors connected to the climate chamber, air temperature and RH were also recorded with sensors (Parrot, Paris, France) installed close to the plant canopy in each climate chamber.

In Exp. 1, conducted in growth chambers for 6 weeks (starting Oct. 26, 2015; Table 1), the variation in whole plant transpiration (ET_c per pot) among cultivars in different climatic conditions was assessed. Based on previous experiments

Table 1 – Plant material and growth conditions applied in different experiments.

Experiment	Facility	Pot rose cultivar	Varying variable	Spacing (pot m^{-2})	Irrigation (%)	RH (day/night %)	Air temperature (day/night °C)	Vapour pressure deficit (day/night kPa)	Light level (μmol m^{-2} s^{-1})	Photoperiod (h)	CO_2 concentration (μmol mol^{-1})	Duration (weeks)	Start date
1	Climate chamber Drought-spotter	'Alaska' 'Aloha' 'Apache' 'Felicitas' 'Flirt' 'Pasadena'	Irrigation RH	25	70 100	60 80	22/18	1.06/0.83 0.53/0.41	300	18	400	6	26 Oct, 2015
2	Climate chamber Drought-spotter	'Alaska' 'Aloha' 'Apache' 'Flirt'	Irrigation	25	60 80 100	80	22/18	0.53/0.41	300	18	400	4	12 Jan, 2016
3	Climate chamber Drought-spotter	'Alaska' 'Aloha' 'Flirt' 'Pasadena'	Irrigation air tempe-rature RH	25	60 100	88/86 (warm) 80/75	26/22 (warm) 18/14	0.4/0.37 0.41/0.40	300	18	400	6	21 Nov, 2016
4	Green-house Weighing-tables	'Alaska' 'Flirt'	Light intensity spacing	25 37.5 50	100	70	21–30/≤17	0.95/0.58	Natural light + Shading or No shading	19	600	6	22 Aug, 2016
5	Green-house Weighing-tables	'Alaska'	RH spacing	25 50	100	30 70	21–30/≤17	2.22/1.36 0.95/0.58	Natural light + SON-T	19	600	6	11 Oct, 2016
6	Green-house Weighing-tables	'Flirt'	RH spacing	25 50	100	30 70	21–30/≤17	2.22/1.36 0.95/0.58	Natural light + SON-T	19	600	9	17 Feb, 2017

Table 2 – Parameters for various stomatal conductance models obtained from non-linear regression over the data of Experiment 6 (see Table 1) with 'Flirt'. Values in the parenthesis are 95% CI of the parameters (d.f. = 52); where $B = P_{nl}\, h_s/(C_s/p_a)$.

Model	Formula	g_0	m_s	a	n	R^2
BWB	$g_s = g_0 + m_s \cdot B$	0.18** (0.13, 0.23)	1.84* (0.45, 3.23)	N/A	N/A	0.12
BWB-Liu	$g_s = g_0 + m_s \cdot e^{n\Psi}B$	0.17** (0.13, 0.21)	6.19** (2.11, 10.23)	N/A	53.50* (7.02, 99.98)	0.31
Modified BWB-Liu	$g_s = g_0 + a \cdot A_s \cdot 10^3 + m_s \cdot e^{n\Psi}B$	0.29** (0.21, 0.37)	8.37** (4.24, 12.50)	−0.16** (−0.26, −0.07)	56.25** (22.64, 89.86)	0.52
	$g_s = g_0 + a \cdot D_s \cdot 10^3 + m_s \cdot e^{n\Psi}B$	−0.10* (−0.21, −0.01)	8.68** (5.85, 11.53)	4.94** (3.24, 6.65)	45.08** (24.33–65.83)	0.59

A – Individual stomatal area (10^3 μm^2); B – Ball index (mol $m^{-2}s^{-1}$); D – Stomatal density (10^3 stomata mm^{-2}); Ψ – Substrate water potential (cm).
*p < 0.5; **p < 0.1 (H_0: coefficient equals 0).

(Giday et al., 2013b, 2015), six commercially available pot rose cultivars with uniform architecture were selected ('Alaska', 'Aloha', 'Apache', 'Felicitas', 'Flirt', and 'Pasadena'). The day/night air temperatures were 22 ± 0.5 °C/18 ± 0.4 °C. Four treatments were applied, consisting of two irrigation regimes (70 and 100% of ET_c, based on well-watered target weight, 330 g) combined with two RH levels (60 and 80% applied over time, see below). Water was supplied to the respective target mass, which was adjusted to account for plant growth [100% being 330 g (week 0–2), 340 g (week 3), 360 g (week 4) and 385 g (week 5–6)]. The RH was set to 60% (weeks 0–2 and 4–6) and 80% (week 3) to induce a different transpiration rate.

In Exp. 2, conducted for 4 weeks (starting Jan. 12, 2016; Table 1), the effect of irrigation regime on plant transpiration was evaluated. Based on Exp. 1, four cultivars with expected large difference in transpiration were selected ('Alaska', 'Aloha', 'Apache' and 'Flirt'). Three treatments were applied based on irrigation regime (60, 80, and 100% of ET_c), adjusted as described in Exp. 1. RH was set to 80% throughout the four-week experimental period, with remaining climate parameters set as in Exp. 1.

In Exp. 3, conducted for 6 weeks (starting Nov. 21, 2016; Table 1), the effect of air temperature on plant transpiration was determined on 'Alaska', 'Aloha', 'Pasadena' and 'Flirt' exposed to various watering regimes. Due to availability restrictions, 'Apache' used in Exp. 2 was replaced with 'Pasadena', which had similar ET_c according to Exp. 1. Four treatments were applied, consisting of two irrigation regimes (60 and 100% of ET_c, adjusted as in Exp. 1) combined with two air temperature levels [26/22 °C (warm), 18/14 °C (cold) for day/night]. RH was adjusted to keep VPD constant among the two air temperature treatments (i.e., the day/night RH was 88/86% in the warm chamber, and 80/75% in the cool chamber), with remaining climate parameters were set as in Exp. 1.

2.1.3. *Greenhouse setup and growth conditions (Exp. 4–6)*

The greenhouse experiments were conducted in 50 m^2 greenhouse compartments fitted with pipe heating connected to a calorifier with ventilator under the tables to prevent climate gradients, and cooling by passive roof ventilation. The climate was controlled by a climate computer (LCC4, Senmatic A/S, Søndersø, Denmark). Air temperature set points were 21 °C with ventilation at 30 °C during daytime, and 17 °C with ventilation at 20 °C at night. RH was set to 70%, maintained by a high-pressure humidification system (Condair Systems, Pfäffikon, Switzerland). The CO_2 concentration was set to 600 μmol mol^{-1}, which was realised by supplying pure CO_2 in the daytime when vents were closed. This carbon dioxide level is common in commercial rose crops. In addition to the climate sensors connected to the climate computer, air temperature and RH were also recorded with sensors (Sensohive Technologies ApS, Odense, Denmark) installed in the upper third of the plant canopy on each weighing table.

The plants were placed on six custom built (0.61 × 1.08 m) ebb-flow tables (Staal & Plast A/S, Ringe Denmark) in a 2 × 3 table pattern in each of two greenhouse compartments with automatic weight registration by single point load cells (1-PW12CC3, HBM, Darmstadt, Germany) connected to data loggers (DataTaker DT85, Thermo Fisher Scientific, Waltham, MA, USA). The irrigation system was constructed with commercially

available components for watering mobile tables (Anderup El, Odense, Denmark), having T-shaped pipes connected to the central watering/fertilisation computer (AMI Completa, Senmatic A/S, Søndersø, Denmark) pumping nutrient solution onto the tables without the pipes contacting the tables, and thus not affecting the weighing. The draining time was controlled by the 4 mm hole in the drain valve and the drain water was collected in gutters under the tables for recirculation via the central watering system. To control the water level on the tables during irrigation, a fully open 15 mm pipe was fitted through the table above the gutter, extended 15 mm above the table surface as overflow drain, when the nutrient solution was pumped up on the table. The plants were given a full nutrient solution automatically adjusted to pH of 6.0 and EC of 2.0 mS cm^{-1} (Fanourakis et al., 2008). Each weighing table was fitted with 35 cm high transparent green plastic filter (LEE Fern Green 122, LEE Filters, Andover, UK) around its perimeter to eliminate the difference in canopy transpiration between tables having one or two outer edges exposed to the surroundings.

In the 6 weeks of Exp. 4 (starting June 14, 2016; Table 1), the effect of light intensity and plant spacing on plant transpiration was determined. Based on Exp. 1, the two cultivars with the largest difference in plant transpiration ('Alaska' and 'Flirt') were chosen. Cultivation took place during the summer period, where solar irradiation potentially reaches the highest annual values. Six treatments were applied, consisting of two light intensity regimes [(1) shading screens (50% shade) unfolded when outside radiation was >500 μmol m^{-2} s^{-1} PPFD; (2) no screens (full sunlight)] without supplementary light, combined by three plant spacing levels (12, 18 and 24 plants per weighing table, i.e., 25, 37.5, and 50 pots m^{-2}). Plants were kept well-watered by using ebb-and-flow irrigation for a 6–9 min period every second day, resulting in water on the tables for ca 12–15 min, depending on plant size.

In Exp. 5 and 6, conducted for 6 and 9 weeks, respectively (starting Oct. 11, 2016 and Feb 17, 2017; Table 1), the effect of RH and plant spacing on plant transpiration was determined on 'Alaska' and 'Flirt', respectively. In both experiments, two RH regimes (30 and 70%) were combined with two plant spacing levels (12 and 24 plants per weighing table, i.e., 25 or 50 pots m^{-2}). From 6:00 to 23:00, supplementary lighting (200 μmol m^{-2} s^{-1} PPFD) was provided at low solar radiation (PPFD < 100 μmol m^{-2} s^{-1}) inside the greenhouse compartment, measured by a quantum sensor (LI-190SA, LI-COR, Lincoln, NE, USA) connected to the climate computer. In both experiments (5 and 6), the remaining climate parameters were set as in Exp. 4.

2.2. Measurements

2.2.1. Biomass and leaf morphological components

In the greenhouse experiments, three pots per cultivar were harvested at day 0, and each week one plant per weighing table was randomly sampled for measurements of leaf area and biomass (see below). The daily plant leaf area was extrapolated from linear connection of the data points of the mean values per cultivar and treatment. Plants that were harvested from the weighing tables were replaced with spare plants grown on an adjacent table with the same plant densities and watering as the weighing tables. All harvest plants were randomly preselected, and all original plants were harvested before the substitute plants were used for harvest.

In all experiments, the final biomass production was assessed. Leaf number and area (leaf area meter LI-3100, LiCor, Lincoln, NE, USA), together with leaf and stem dry masses were recorded after drying the plant tissue for at least 48 h at 80 °C in a drying oven (Seif et al., 2021). The specific leaf area (SLA; leaf area/leaf mass) was calculated. The measurements were conducted on three plants per weighing table (Exp. 3 and 4) or four plants per treatment (Exp. 1, 2, 5 and 6).

The effect of growth environment on stomatal pore length (major axis), pore aperture (minor axis), and D_s was determined. *Rosa x hybrida* has compound leaves, where leaflets arise on both sides of the rachis (i.e. in pairs) besides the terminal leaflet (odd-pinnate arrangement). Measurements were carried out on one leaflet of the first pair of lateral leaflets from the first order pentafoliate leaf (counting from the apex). The silicon rubber impression technique was employed [elite HD+, Zhermack, Badia Polesine, Italy (Fanourakis, Giday, et al., 2019)]. Imprints were made 2 h following the onset of the light period, since this time is required for plants exposed to prolonged darkness (i.e. night time period) to reach steady-state stomatal aperture. The sampling area (1 × 1 cm) was located midway between the leaflet base and tip, and between the midrib and lateral margin (Fanourakis, Hyldgaard, et al., 2019; Sørensen et al., 2020). The fields of view were located in interveinal areas, since veins lack stomata (Fanourakis et al., 2015). Images were acquired using an optical microscope (Leitz Aristoplan; Ernst Leitz Wetzlar GmbH, Wetzlar, Germany) connected to a digital camera (Nikon DXM-1200; Nikon Corp., Tokyo, Japan). The rose is a hypostomatous species (Fanourakis et al., 2015), so only the abaxial leaflet surface was assessed. Stomatal pore length and aperture were determined on ten randomly selected stomata (magnification × 200), while D_s was counted on five non-overlapping interveinal fields of view per leaflet (magnification × 100). A_p was calculated as the area of an ellipsis with major and minor axes being the pore length and pore aperture, respectively [i.e., $A_p = \pi \times \left(\frac{\text{pore length}}{2}\right) \times \left(\frac{\text{pore aperture}}{2}\right)$]. Image processing was performed with ImageJ software (https://imagej.nih.gov/, Koubouris et al., 2018; Fanourakis et al., 2021). Three (Exp. 5 and 6) or four (Exp. 2 and 3) leaflets were assessed per treatment.

2.2.2. Stomatal conductance (g_s)

The effect of environmental conditions on g_s was examined by porometry. *In situ* g_s measurements were done on attached leaves of intact plants. The g_s was determined with a Decagon SC-1 porometer (Meter Group, Inc., Pullman, WA, USA). Evaluations took place 2 h after the onset of the light period to ensure steady-state g_s with open stomata (Fanourakis et al., 2017). Three measurements on different leaves per plant were performed. Three (Exp. 4, 5 and 6) or four (Exp. 1, 2, and 3) plants per treatment were assessed. Measurements were done once per week starting on week 3 (Exp. 1–3) or three times per week during the last cultivation week (Exp. 4–6).

2.2.3. Plant transpiration

The effect of growth environment on whole plant transpiration was evaluated during growth. For the growth chamber

experiments (1–3) the water loss of individual pots was (automatically) determined by the mass difference in 5-min intervals using the two Drought Spotter units, each containing 24 single pot balances (Fanourakis et al., 2017). Growing-media evaporation rate was assessed in three (Exp. 1) or five (Exp. 2, and 3) pots without plants, but with identical media water content as in pots with plants after a duration of four days with treatment. Direct evaporation from the media was subtracted from pot water loss to determine plant water loss (Fanourakis et al., 2017, 2019a, 2019b). Treatments were compared based on the average transpiration rate over the complete assessment period.

For the greenhouse experiments (4–6), the canopy water loss of a 0.61 × 1.08 m canopy was determined by the previously described weighing tables, where the mass was logged every 3 min. The plants were watered daily at 07:00, and the transpiration rate was calculated as the slope of the water loss over time from 11:00 to 16:00, since the transpiration curve was linear in this time interval and unaffected by the watering.

In all cases, transpiration rate was calculated as per plant for the last five days of the experimental periods.

2.3. Model

2.3.1. Plant transpiration model

Evapotranspiration of a single plant was modelled as the sum of evapotranspiration of all leaves of that plant, and then it was up-scaled to the crop level for simulations. For vertical leaf distribution (within-plant or within-plant stand) and microclimate differences, the approach of separating the plant or crop into three horizontal layers was employed (described by Körner et al., 2007). Stomatal conductance was calculated for individual leaves with four different options: (1) the BWB-model (Ball et al., 1987), (2) the BWB-Liu-model (Liu et al., 2009), or (3, 4) the two adjusted versions of BWB-Liu-model (by employing A_p and D_s, respectively).

The empirical BWB-model as used by Kim and Lieth (2003) uses leaf net photosynthesis rate (P_{nl}), air CO_2 partial pressure (C_s), and h_s (leaf surface RH fraction) as driving variables:

$$g_s = g_0 + m_s P_{nl} \frac{h_s}{(C_s/p_a)} \quad (1)$$

where g_0 is the leaf minimum (residual) g_s as P_{nl} reaches 0, while m_s is an empirical coefficient for the sensitivity of g_s to P_{nl}; m_s includes the empirical scaling to mol.

Practically, the BWB-model describes the correlation of g_s with physiological CO_2 assimilation and vice versa. P_{nl} is input for the g_s calculation, while inversely g_s is input for the P_{nl} calculation. This clustering of two sub-models (with interdependent input and output) demands start values and iteration in simulation.

The BWB-Liu-model uses substrate water potential (Ψ) to explain the fluctuation of the slope (m_s). The average pot mass (obtained from the weighing tables) was converted into Ψ, by using the Van Genuchten equation (Van Genuchten, 1980) with saturated water content (θ_s), the residual water content (θ_r; assumed to be 0), and the two dimensionless constants m_g and n_g. The effective water content (θ/θ_s) was obtained by using Equation (2). The volumetric water content (θ) was obtained from linear least squares' regression by the empirical Equation (3) (using the fresh and dry pot mass data; w_{pf}, w_{pd}, respectively; Exp. 6), where c is the correction of measuring errors.

$$\frac{\theta - \theta_r}{\theta_s - \theta_r} = \left[1 + |\beta\Psi|^{n_g}\right]^{m_g} \quad (2)$$

$$\theta = -0.203 + 0.00225 \times w_{pf} + c \quad (3)$$

P_{nl} was obtained by fitting the negative exponential light response curve (Thornley, 1976, p. 318) with leaf photochemical efficiency (α_l, [mol CO_2] [mol photons]$^{-1}$) and maximum leaf net photosynthesis ($P_{nl,max}$, μmol m^{-2} s^{-1}) for the different canopy levels (z) according to the PPFD (μmol m^{-2} s^{-1}). Absorbed PPFD values were calculated separately for diffuse and direct radiation and as function of z (Van Kraalingen & Rappoldt, 1989). Parameters α_l and $P_{nl,max}$ were calculated based on a combined method of biochemical leaf photosynthesis models (Farquhar et al., 1980; Farquhar & Von Caemmerer, 1982) and approaches of Gijzen (1994), as shown by Körner (2004).

We have investigated the extension of the BWB and the BWB-Liu models with A_p or D_s. All models [(1) BWB, (2) BWB-Liu, (3, 4) BWB and BWB-Liu extended with A_p, and (5, 6) BWB and BWB-Liu extended with D_s] were parameterised using data sets from both experimental measurements (leaf g_s, leaf temperature, w_{pd}), environmental variables (air temperature, h_s, and PPFD) of Exp. 4–6 or model calculations (P_{nl}).

2.3.2. Model parameterisation and implementation

For comparison of the two cultivars with extreme differences in potential ET_c ('Alaska' and 'Flirt'), the two parameters of the BWB-model (m_s and g_0) were parameterised with the fit procedure with non-linear least squares of the mathematical software environment MATLAB (ver. R2020a, The MathWorks, Inc., Nattics, USA). The parameterised BWB g_s-model was implemented as sub-model in a crop microclimate and evaporation model (Körner et al., 2007) and validated as major driver for ET_c. As such, the model was validated with measured ET_c data obtained in Exp. 4 for the cultivars 'Alaska' and 'Flirt' with three plant spacing levels (12, 18 and 24 plants m^{-2}) for an 11-d period each. For simulations, the crop specific parameters for pot rose and measured greenhouse climate data (3-min interval; temperature, RH, CO_2 concentration, and PPFD) were used as input to the model. Climate data were recorded with a combination of sensors (Sensohive Technologies ApS, Odense, Denmark; Parrot, Paris, France) installed close to the plant canopy. The cultivar specific parameters of the g_s model were the only difference between the two cultivars as implemented in the ET_c model.

For the data of Exp. 6, the CO_2 concentration was set constant at 600 ppm and the BWB model, the BWB-Liu, and the two extended BWB-Liu models were further parametrised for 'Flirt' by fitting the observed data with the mathematical software environment R (The R Project, r-project.org) using non-linear least squares method [nls()] and model prediction performance with linear regression analysis [lm()].

2.3.3. Simulation study

After validation of the g_s model (parameterised with two opposite reacting rose cultivars; 'Alaska' and 'Flirt') as a sub-model in an ET_c model, the ET_c model was further implemented in an existing greenhouse simulator (Goddek & Körner, 2019; Körner & Hansen, 2012) as implemented in HORTSIM v.0 (Körner & Holst, 2017). The simulator consists of a complete set of physical, biological and crop specific sub-models, including a replica of a commercially-used climate controller. A standard multi-span greenhouse (1-ha floor area) with standard equipment for heating (pipes), ventilation (roof vents), screening (energy and shading), and supplementary lighting (max. 60 W m^{-2} high pressure sodium lamps) as well as set points for climate control of pot roses was used. Copenhagen (Denmark) was selected as location, and a data set of hourly values for a standard climate year in Denmark (Wang et al., 2013) was used. For climate control, set points for all actuators were calculated based on basic set points and climate inside and outside the greenhouse (as in commercial practise) e.g. heating and passive roof ventilation for temperature and RH control. Individual simulations with two cultivars ('Flirt' and 'Alaska'; all other parameters and conditions remained the same) were undertaken for a 365 d period with a 5 min time step, and integrated for each 60 min. Eight climate scenarios with different RH set points (ranging between 65% and 100%) were performed. Output from the simulations included hourly values of g_s, greenhouse macro and microclimate variables (e.g. leaf temperature in three layers), ET_c, as well as overall greenhouse energy household and demand.

2.4. Data analysis and statistics

All data analyses were performed with the mathematical software package Matlab (ver. R2020a; The MathWorks Inc.) incl. *Curve Fitting Toolbox* and *Statistics and Machine Learning Toolbox*. Statistical analyses were performed with analysis of variance (ANOVA) followed by a post-hoc test applying the Tukey's HSD test (Tukey–Kramer) on the alpha level 0.05 using the procedures *anovan* and *multcompare*. Parameter estimation of the BWB, BWB-Liu and the extended versions of the BWB-Liu model was done with non-linear least square estimation (*nlinfit* and *fit* procedures).

3. Results

3.1. Plant experiments

3.1.1. Cultivar screening for ETc

Six pot rose cultivars were screened in Experiment 1. Leaf area (range: 0.17–0.27 m^2 $plant^{-1}$; Fig. 2A), SLA (range: 220–280 cm^2 g^{-1}; Fig. 2B), g_s (range: 290–410 mmol m^{-2} s^{-1}; Fig. 2C) and ET_c (range: 1–1.2 L $plant^{-1}$; Fig. 2D) varied among the cultivars under study. 'Flirt' and 'Aloha' as representatives of lower g_s and ET_c, and 'Alaska' and 'Apache' as representative of higher g_s and ET_C (Fig. 2C, D) were selected for Exp. 2. In those pairs, 'Aloha' had higher leaf area and smaller SLA than 'Flirt', and 'Apache' both larger leaf area and higher SLA than 'Alaska' (Fig. 2A, B).

Increasing RH (from 60 to 80%) and/or irrigation (from 70 to 100%) led to enhanced g_s in all studied cultivars (Table 3).

3.1.2. Effect of irrigation level on g_s and ET_c

In Exp. 2, cultivar differences in leaf area were similar to Exp. 1 (Fig. 3A). 'Alaska' and 'Flirt' had the thickest and thinnest leaves with 218 and 287 cm^2 g^{-1}, respectively (as indicated by SLA, Fig. 3B). Similarly to Exp. 1, 'Flirt' and 'Aloha' had lower g_s, as compared to 'Alaska' and 'Apache' (Fig. 3C).

A slight increase, owing to irrigation regime, was noted for leaf area (Fig. 4A) and SLA (Fig. 4B) in all four cultivars. While g_s generally decreased with increased irrigation (100 as compared to 60%) in 'Aloha' and 'Flirt', a minor effect was observed for 'Apache' and 'Alaska' (100 as compared to 60%; Fig. 4C). However, the increased irrigation generally led to a higher ET_c in all cultivars but 'Flirt' (Fig. 4D).

3.1.3. Effect of temperature (combined with RH) on g_s and ET_c

Based on the screening experiments (1 and 2), two cultivars ('Flirt' and 'Alaska') with extreme differences in ET_c were selected for further analyses. The cultivation temperature (combined with RH to maintain a stable VPD) had only a minor effect on plant leaf area (Fig. 5A), while SLA decreased with increasing temperature in both cultivars (Fig. 5B). Instead, higher temperature enhanced both g_s (Fig. 5C) and ET_c (Fig. 5D). The effect of temperature on g_s was more pronounced in 'Flirt' than in 'Alaska' (Fig. 5C). In contrast to the expected from increased g_s and ET_c with rising temperature, a higher temperature led to decreased stomatal pore aperture (Fig. 6A), pore length (Fig. 6B), and density in both cultivars (Fig. 6C).

3.1.4. Effect of plant density on g_s and ET_c

Plants were harvested at 7 or 14 d after the start of experiment, when plants were just after second cut. For either harvest date, the effect of plant density on plant leaf area was generally limited and not consistent among cultivars (Fig. 7A). Instead, increasing plant density clearly led to enhanced SLA (Fig. 7B). As the plants grew and the canopy closed, increasing plant density also led to a consistent increase of g_s from cultivation day 6 and onwards (Fig. 8).

3.1.5. Effect of RH on g_s and ET_c

Increasing the set point of RH (from 30 to 70%) resulted in significantly different greenhouse climate (data not presented). The high RH (i.e. low VPD) led to both increased g_s (Fig. 9A) and decreased ET_c (Fig. 9B). Leaves developed at high RH had significant larger A_p (Fig. 10A), while D_s was not significantly different (Fig. 10B), as compared to leaves developed at low RH.

3.2. Model and simulations

3.2.1. BWB-model parameterisation and validation

The BWB model was parametrised with data from Exp. 5 for the two cultivars 'Flirt' and 'Alaska' with and without additional term for CO_2 concentration (Table 4). Modelled g_s ($g_{s,sim}$) was then implemented in an ET_c model (Körner et al. 2007) and a validation study comparing $g_{s,sim}$ with measured g_s ($g_{s,meas}$) on an independent data-set was performed. For that,

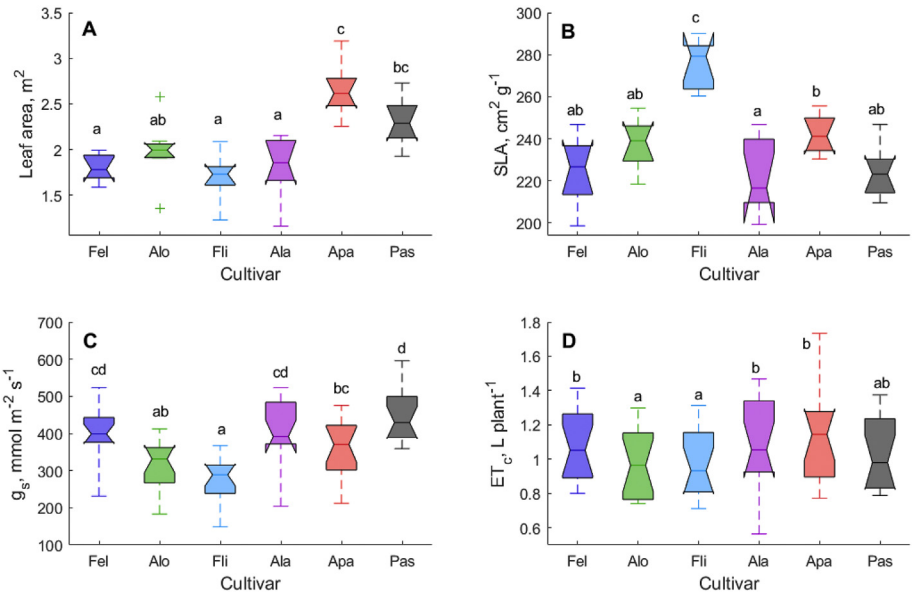

Fig. 2 – Plant leaf area (A), specific leaf area (SLA; B), stomatal conductance (g_s; C) and evapotranspiration rate (ET_c; D) of six pot rose cultivars ('Felicitas', Fel; 'Flirt', Fli; 'Aloha', Alo; 'Alaska', Ala; 'Apache', Apa; 'Pasadena'; Pas) in Exp. 1 (see Table 1). Data of the four treatments were pooled. Whisker (W) was set to 2.5, and points were drawn as outliers if they were larger than $Q_{25}+W*(Q_{75}-Q_{25})$ or smaller than $Q_{25}-W*(Q_{75}-Q_{25})$. Different letters indicate statistically significant difference (alpha 0.05) with Tukey's HSD test (Tukey–Kramer).

Table 3 – Stomatal conductance of six pot rose cultivars in Experiment 1 (see Table 1). Plants were grown under two watering levels (70, 100%) and at moderate (60%) or high (80%) relative air humidity (RH). RH was set to 60% (0–2 and 4–6 weeks) or 80% (3rd week), depending on the week of growth. Measurements were conducted in the growing environment and on intact plants 2 h following the onset of the light period (n = 3). Standard deviation is indicated in brackets.

Cultivar	Stomatal conductance (mmol m^{-2} s^{-1})			
	Treatment [watering regime (%)/RH (%)]			
	100/60	70/60	100/80	70/80
Alaska	390 (38)	304 (85)	488 (35)	444 (66)
Aloha	291 (55)	200 (37)	321 (38)	295 (25)
Apache	347 (43)	271 (42)	439 (29)	414 (36)
Felicitas	398 (33)	329 (69)	482 (34)	414 (25)
Flirt	326 (58)	233 (38)	369 (37)	342 (27)
Pasadena	434 (27)	383 (17)	545 (47)	430 (61)

ET_c of the two cultivars with three plant densities (12, 18, 24 plants m^{-2}) was used (Exp. 4). Generally, a very good agreement between simulated and measured ET_c was noted, while the effect of plant density on ET_c was also very well approximated by using the model (Fig. 11). It was clear that a higher plant density lowered plant ET_c. At the lowest plant density (12 plants m^{-2}), a slight underestimation of ET_c was observed, and the model slightly underestimated the cultivar differences in ET_c (Fig. 11).

3.2.2. *Model extension*

As first step, the BWB-model was extended with A_p for the cultivar 'Flirt' in order to analyse the effect on improved fitting quality by adding an extra dynamic parameter. For that, this extended BWB-model was compared to measurements of Exp. 5 with two RH set-point levels (30, 70%) independently. The extension resulted in only a small difference to the original model (Fig. 12). In both model cases, a poor fit to measured g_s was observed at low humidity levels (R^2 of 0.275 or 0.268), while at higher RH levels the fit for the two model versions was rather good (R^2 of 0.765 or 0.766; Fig. 12C,D).

It was concluded that the current model was not capable of predicting g_s at low RH with and without the extension of a dynamic A_p, as it does not adequately take the greenhouse climate dynamics into account: in addition to the climate variables CO_2 and RH, it employs only one single variable (P_{nl}), incorporating the plant physiological responses to all climate variables. To improve the prediction quality at low RH levels and under dynamic climate conditions, the BWB-Liu model that includes substrate Ψ as additional variable was therefore used in the next step, extended and parameterised with data of Exp. 6 for 'Flirt'. Four versions of the BWB-model were compared: (1) BWB-model, (2) BWB-Liu-model, (3) modified BWB-Liu-model by employing A_p, and (4) modified BWB-Liu-model by employing D_s (Fig. 13). In this parameterisation procedure, the complete climate data set with all RH values was used. As expected from Exp. 5 fittings, the model quality predicting g_s was poor when the basic BWB-model was used (R^2 = 0.12, Fig. 13A, Table 2). The BWB-Liu-model, which was extended with Ψ, performed better, though the R^2 was still low (0.31; Fig. 13B; Table 2). Instead, by modifying the BWB-Liu-model further by adding stomatal features allowed much higher accuracy in estimating g_s. When adding A_p, R^2 increased to 0.52 (Fig. 13C, Table 2), while adding D_s improved it to 0.59 (Fig. 13D; Table 2). The extensions are thus capable of overcoming the weak model behaviour at low RH levels. At

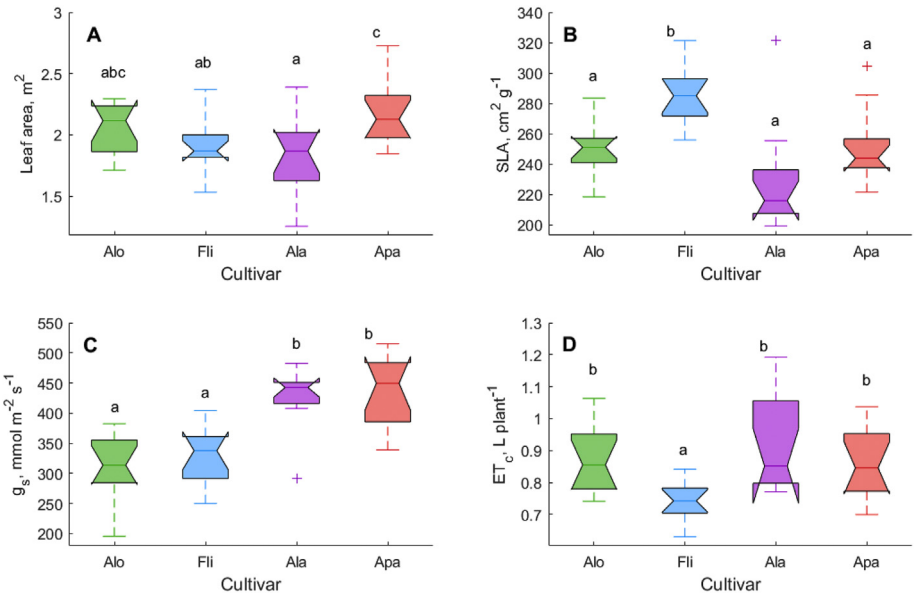

Fig. 3 – Plant leaf area (A), specific leaf area (SLA; B), stomatal conductance (g_s; C) and evapotranspiration rate (ET_c; D) of four pot rose cultivars ('Apache', Apa; 'Alaska', Ala; 'Aloha', Alo; 'Flirt', Fli) in Exp. 2 (see Table 1). Data of the three treatments were pooled. Whisker (W) was set to 2.5, and points were drawn as outliers if they were larger than $Q_{25}+W*(Q_{75}-Q_{25})$ or smaller than $Q_{25}-W*(Q_{75}-Q_{25})$. Different letters indicate statistically significant difference (alpha 0.05) with Tukey's HSD test (Tukey–Kramer).

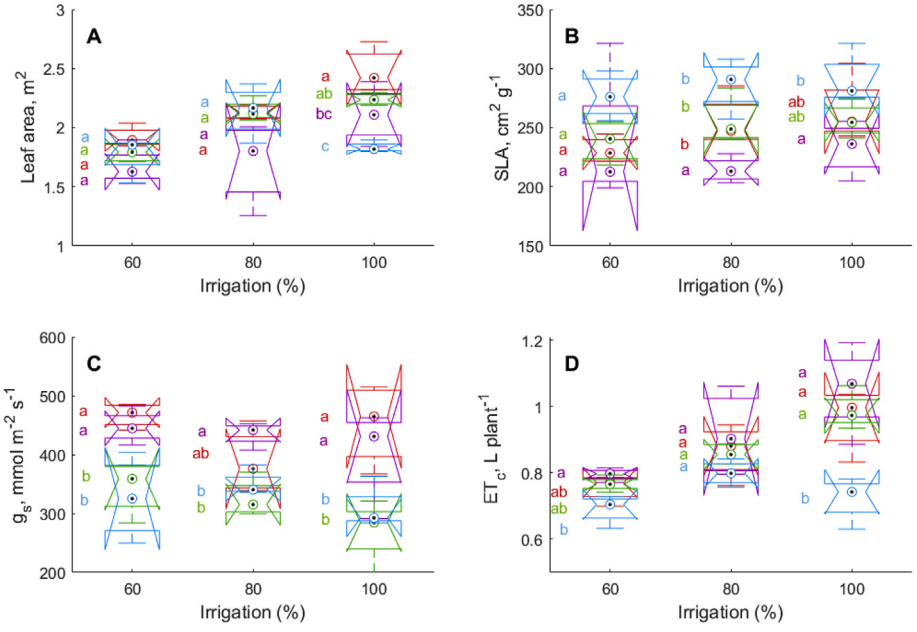

Fig. 4 – Effect of irrigation regime on plant leaf area (A), specific leaf area (SLA; B), stomatal conductance (g_s; C) and evapotranspiration rate (ET_c; D) of four pot rose cultivars ('Aloha', green; 'Flirt', cyan, 'Alaska', magenta; 'Apache', red) in Exp. 2 (see Table 1). Whisker (W) was set to 2.5, and points were drawn as outliers if they were larger than $Q_{25}+W*(Q_{75}-Q_{25})$ or smaller than $Q_{25}-W*(Q_{75}-Q_{25})$. Different letters indicate statistically significant difference between cultivars in each irrigation level (alpha 0.05) with Tukey's HSD test (Tukey-Kramer). (For interpretation of the references to colour in this figure legend, the reader is referred to the Web version of this article.)

higher RH levels (approximately >60%) the BWB-model, however, is a useful and simple predictor of g_s without the necessity of additional input of stomatal traits or Ψ, which are accessed with difficulty.

3.2.3. *Greenhouse climate control simulations*

Despite the improvements in model predictions with the extended BWB-Liu model versions, the parameterisation of the BWB-Liu model and the extensions is difficult in practise.

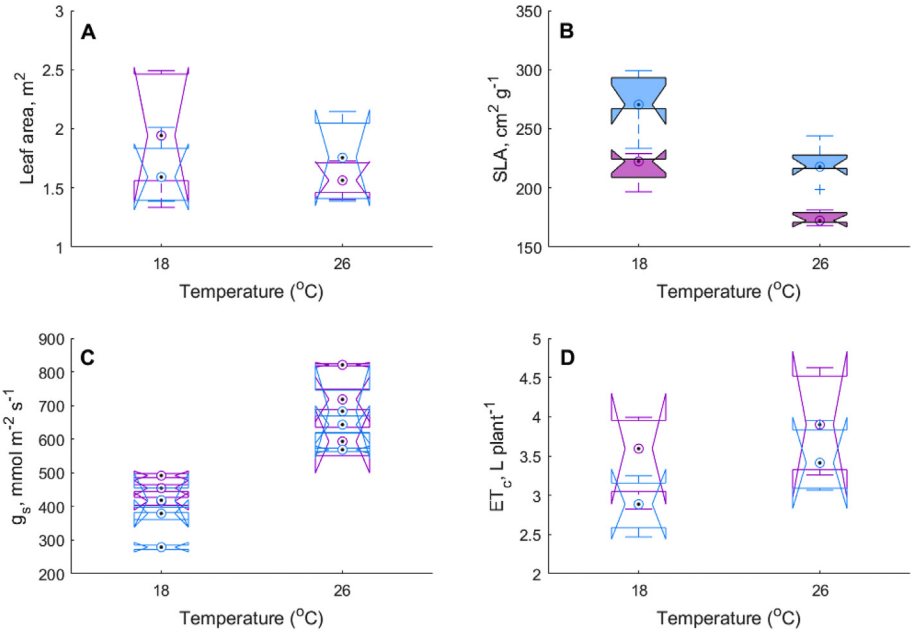

Fig. 5 – Effect of temperature (combined with relative air humidity) on plant leaf area (A), specific leaf area (SLA; B), stomatal conductance [g_s; includes data of three dates (23.12, 29.12, and 04.01); C] and evapotranspiration rate (ET_c; D) of the two most contrasting pot rose cultivars ('Alaska', magenta; 'Flirt', cyan) in Exp. 3 (see Table 1). Data of two irrigation treatments were pooled. Whisker (W) was set to 2.5, and points were drawn as outliers if they were larger than $Q_{25}+W*(Q_{75}-Q_{25})$ or smaller than $Q_{25}-W*(Q_{75}-Q_{25})$. (For interpretation of the references to colour in this figure legend, the reader is referred to the Web version of this article.)

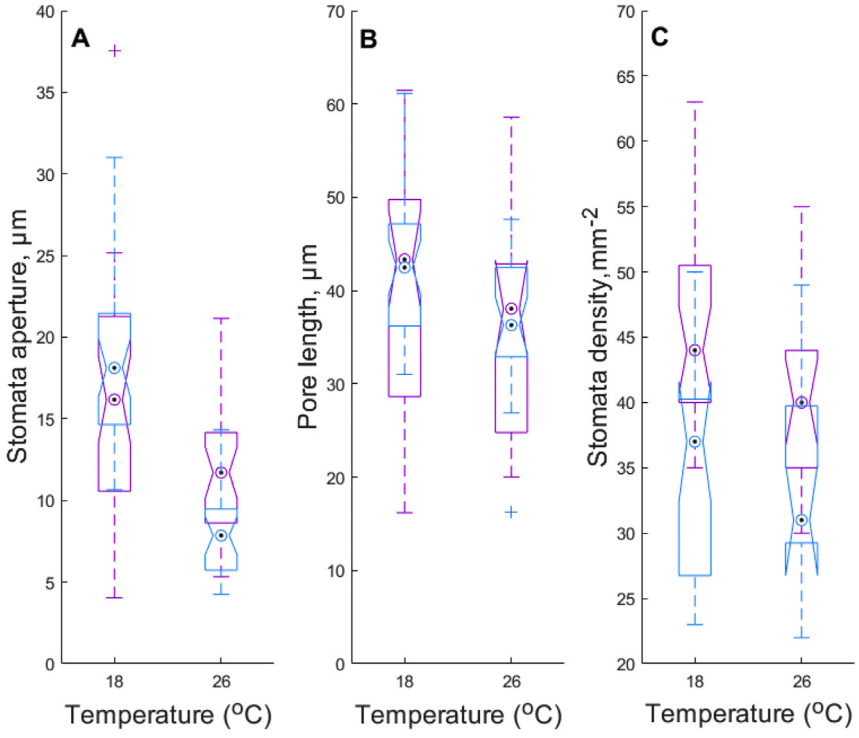

Fig. 6 – Effect of temperature (combined with relative air humidity) on stomatal pore aperture (A), stomatal pore length (B), and stomatal density (C) of the two most contrasting pot rose cultivars ('Alaska', magenta; 'Flirt', cyan) in Exp. 3 (see Table 1). Data of two irrigation treatments were pooled. Whisker (W) was set to 2.5, and points were drawn as outliers if they were larger than $Q_{25}+W*(Q_{75}-Q_{25})$ or smaller than $Q_{25}-W*(Q_{75}-Q_{25})$. (For interpretation of the references to colour in this figure legend, the reader is referred to the Web version of this article.)

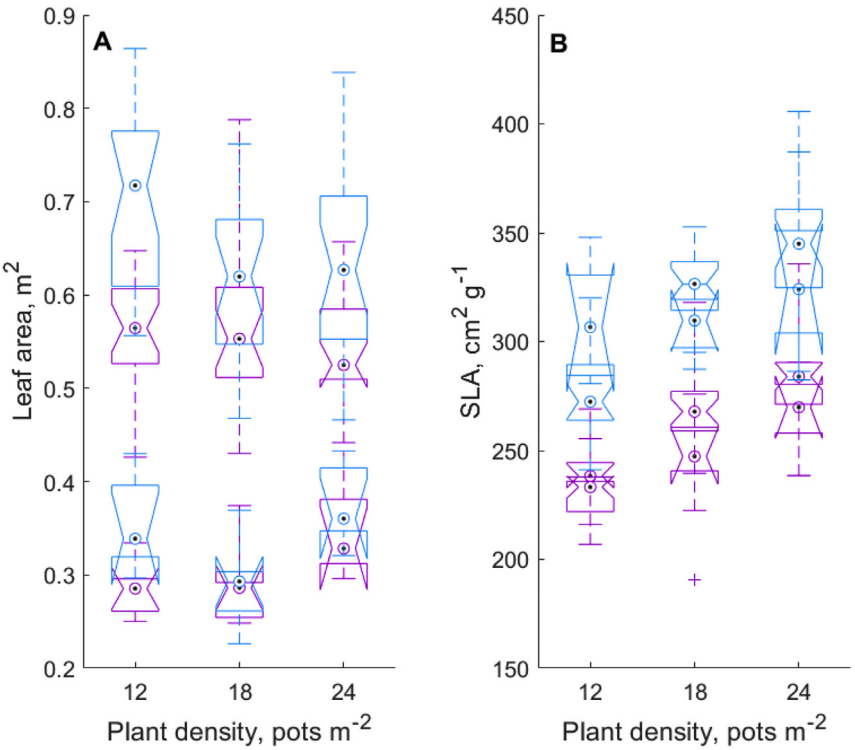

Fig. 7 – Effect of planting density on leaf area (A), and specific leaf area (SLA; B) at 7 (lower boxplots) and 14 (upper boxplots) days after the start of experiment (after second cut) of two most contrasting pot rose cultivars ('Alaska', magenta; 'Flirt', cyan) in Exp. 4 (see Table 1). Data of two light intensity treatments were pooled. Whisker (W) was set to 2.5, and points were drawn as outliers if they were larger than $Q_{25}+W*(Q_{75}-Q_{25})$ or smaller than $Q_{25}-W*(Q_{75}-Q_{25})$. (For interpretation of the references to colour in this figure legend, the reader is referred to the Web version of this article.)

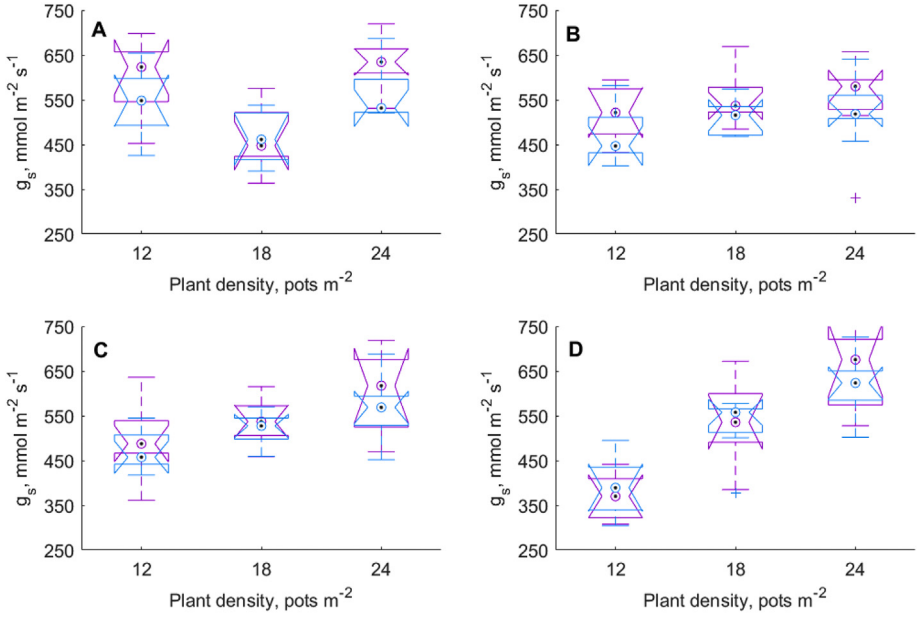

Fig. 8 – Effect of planting density on stomatal conductance (g_s) at 2 (A), 6 (B), 10 (C), 12 (D) days after the start of experiment (after second cut) of two most contrasting pot rose cultivars ('Alaska', magenta; 'Flirt', cyan) in Exp. 4 (see Table 1). Data of two light intensity treatments were pooled. Whisker (W) was set to 2.5, and points were drawn as outliers if they were larger than $Q_{25}+W*(Q_{75}-Q_{25})$ or smaller than $Q_{25}-W*(Q_{75}-Q_{25})$. (For interpretation of the references to colour in this figure legend, the reader is referred to the Web version of this article.)

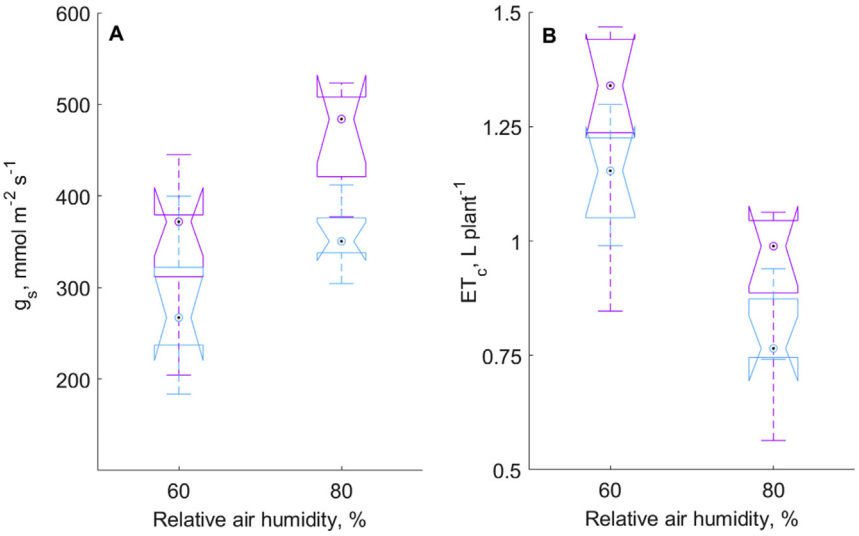

Fig. 9 – Effect of relative air humidity on stomatal conductance (g_s; A) and evapotranspiration rate (ET_c; B) of two most contrasting pot rose cultivars ('Alaska', magenta; 'Flirt', cyan) in Exp. 1 (see Table 1). Whisker (W) was set to 2.5, and points were drawn as outliers if they were larger than $Q_{25}+W*(Q_{75}-Q_{25})$ or smaller than $Q_{25}-W*(Q_{75}-Q_{25})$. (For interpretation of the references to colour in this figure legend, the reader is referred to the Web version of this article.)

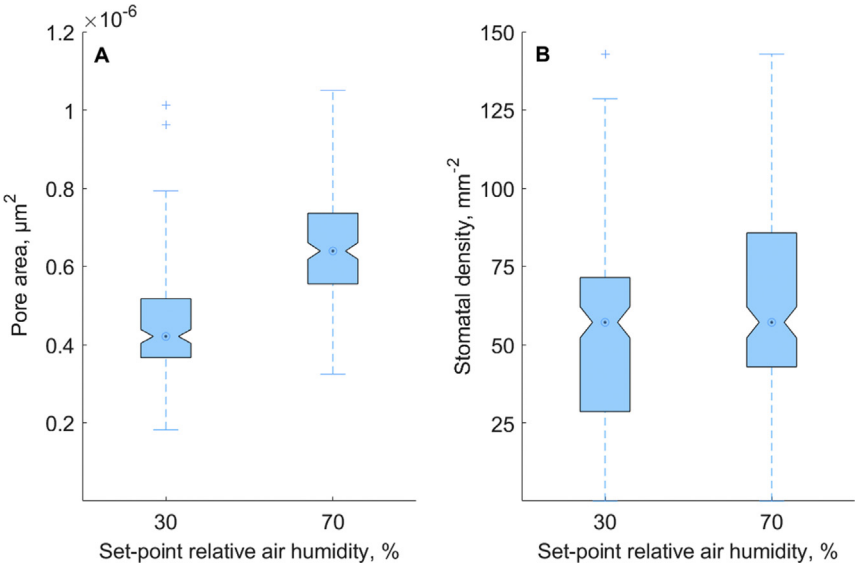

Fig. 10 – Effect of relative air humidity on stomatal pore area (A) and stomatal density (B) of cv. 'Flirt' in Exp. 5 (see Table 1). Data of two spacing treatments were pooled. Whisker (W) was set to 2.5, and points were drawn as outliers if they were larger than $Q_{25}+W*(Q_{75}-Q_{25})$ or smaller than $Q_{25}-W*(Q_{75}-Q_{25})$. Different letters indicate statistically significant difference (alpha 0.05) with Tukey's HSD test (Tukey–Kramer).

As the simple BWB-model performs well under high RH levels, the implications of cultivar differences in g_s for the greenhouse energy household was therefore quantified with the simple BWB-based ET_c model using a range of elevated RH levels (with 65% as lowest). The comparative simulation study between the two cultivars 'Alaska' and 'Flirt' is illustrated in Fig. 14. Simulations showed that 'Flirt' has a consistently lower g_s as compared to 'Alaska' (Fig. 14A) and a general decrease in latent heat production (measure for ET_c) was observed when increasing the RH set point (Fig. 14B). The relative difference in ET_c between 'Flirt' and 'Alaska' was highest at lowest RH set point, while the difference decreased with increasing the RH set point (Fig. 14C; absolute difference in Fig. 14D).

The relative difference in energy demand between 'Flirt' and 'Alaska' was approximately 1% for 65%–75% RH, and between 2.35 and 5.75% for 85%–95% RH (Fig. 14E; absolute difference in Fig. 14F), peaking at the RH set point of 90%. As

Table 4 – Fitted parameters of the Ball–Berry stomatal conductance model (BWB-model) obtained from non-linear regression with of data of Experiment 4 (see Table 1) with pot rose cultivars 'Flirt' and 'Alaska'. [g_0, minimum (residual) g_s as leaf net photosynthesis rate reaches 0; m_s, adjustment factor at 400 μmol mol^{-1} CO_2 (m_s) and as function of variable CO_2 $m_{s[CO2]}$].

Cultivar	g_0	m_s	$m_{s[CO2]}$
Alaska	0.1036	3.810	0.01016 [CO_2]
Flirt	0.0759	4.646	0.01239 [CO_2]

expected, due to the lack of RH control at a set point of 100%, no difference in heating energy consumption between the two cultivars was observed (Fig. 14E, F).

4. Discussion

In the current study, g_s was measured employing a set of six pot rose cultivars and a wide range of climate conditions (varying RH, irrigation, temperature, light level and planting density; Table 1), and results were utilised to improve the coupling of estimated and actual ET_c (Fig. 1), and in turn contribute to the energy saving potential. This study reveals the necessity of cultivar specific g_s models for improved estimations of ET_c, and in this way enhanced climate management. By using a cultivar specific parameter set within an ET_c model, the ET_c of individual cultivars could be more accurately estimated during cultivation.

4.1. *Low g_s genotypes improve energy saving related to RH control*

In greenhouse production, reduced energy use has become increasingly important. A more efficient RH control, is important since it represents a principal energy flow and has consequences for growth, production, and quality of the produce. Our study clearly indicates that manipulating g_s directly affects energy demand related to RH control. Selecting low-g_s cultivars reduces annual energy demand (2.5–5.75% depending on the RH set point; Fig. 14E, F). As economic benefits are considerable due to the high share of energy costs in moderate and cool climate greenhouse production, and since the proposed methodology can be implemented without additional investments, this approach certainly deserves further exploration.

Arguably g_s is an unexploited trait in ongoing breeding programs. Breeding programs should consider overall steady state g_s value as a parameter critical to cultivation management and costs (Fig. 14). Besides this critical benefit, a growing body of evidence also suggests that decreased g_s also contributes to prolonged postharvest longevity (Carvalho et al., 2016; Fanourakis et al., 2016b, 2020b). However, successful utilisation of a selection trait in breeding programs requires a robust non-invasive methodology, which is suitable for large-scale plant analyses. Measurements of leaf and canopy temperature by thermal imaging have been successfully introduced to evaluate overall g_s (Kohtaro & Olajumoke, 2020).

Potentially commercially important genetic variation in g_s was found in a small set of commercial pot rose cultivars (Fig. 2) as it is evident in a range of other species (Medlyn et al.,

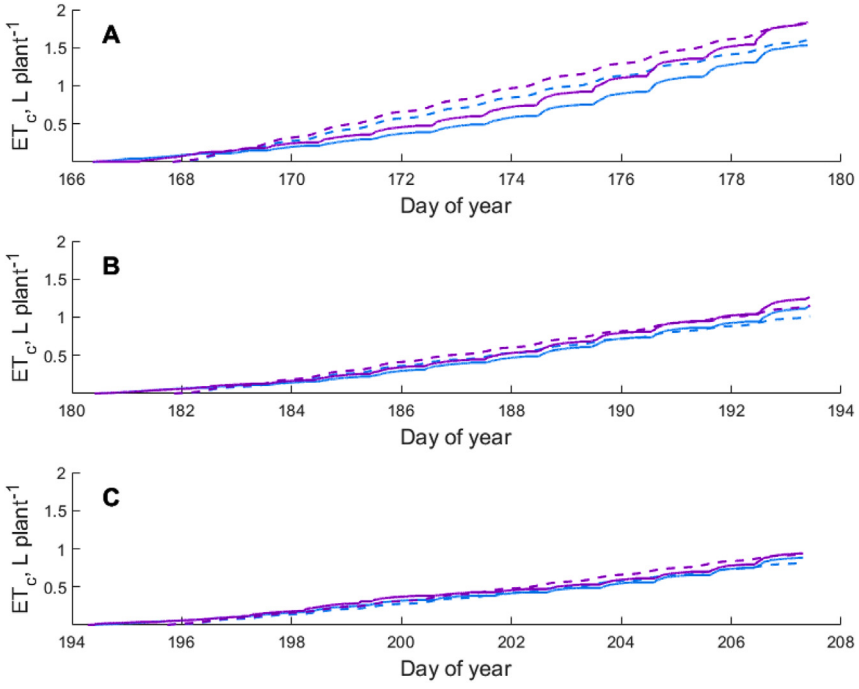

Fig. 11 – Simulated (dashed lines) versus measured (solid lines) plant evapotranspiration (ET_c) for three plant densities [12 (A), 18 (B) and 24 (C) plants m^{-2}] of two most contrasting pot rose cultivars ('Alaska', magenta; 'Flirt', cyan) in Exp. 5 (see Table 1). The differences in the x-axes should be noted as different start dates for the different spacings. (For interpretation of the references to colour in this figure legend, the reader is referred to the Web version of this article.)

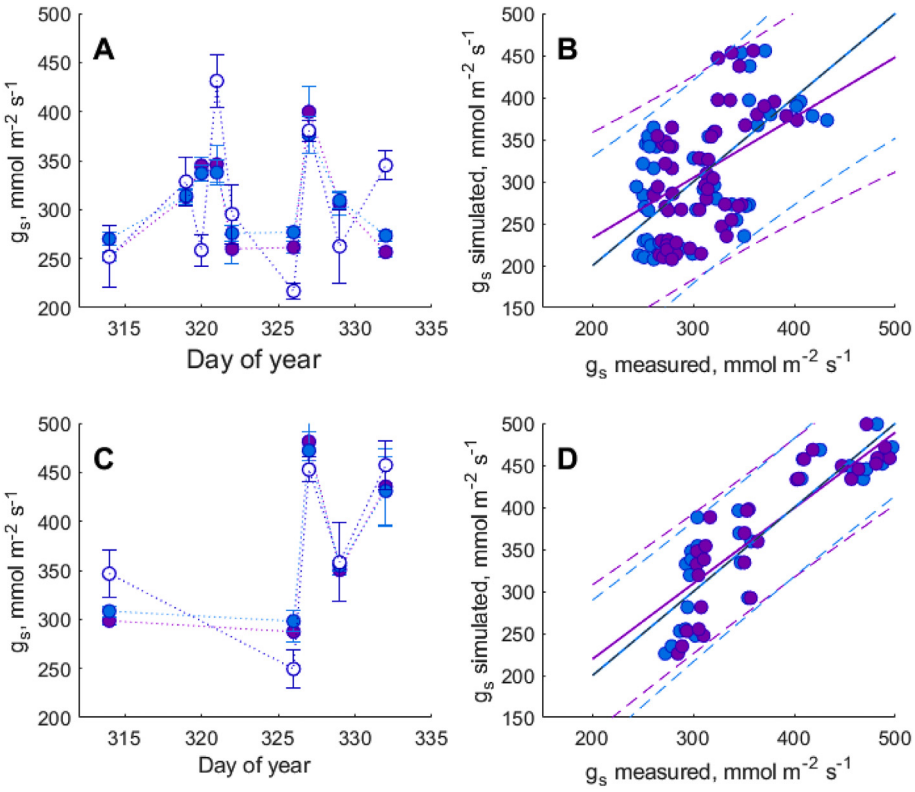

Fig. 12 – Observed versus predicted stomatal conductance (g_s) in the cultivar 'Flirt' in Exp. 5 at 30% (A, B) or 70% (C, D) relative air humidity setpoints (RH) by using the BWB model (light blue) and the BWB model with an additional function for individual stomatal pore area with R^2 of 0.275 or 0.268 at 30% RH; 0.765 or 0.766 at 70% RH (magenta) compared to measured g_s (A, C; blue stars). (For interpretation of the references to colour in this figure legend, the reader is referred to the Web version of this article.)

2011; Merilo et al., 2014). This variation in g_s was reasonably persistent across different experiments (Figs. 2, 3, 5 and 8). The range in ET_c of these cultivars was also similar to that recorded in previous studies (Giday et al., 2013b, 2015), with the difference between the lowest and highest ET_c being about 20% (Fig. 2D). The rankings and the magnitude of cultivar differences in g_s and ET_c cited here may differ from those that could occur under persistent abiotic stress, such as water deficit (Giday et al., 2014) or saline conditions (Hassanvand et al., 2019). However, the cultivar effects on g_s in the absence of stress are mostly relevant in protected cultivation.

Evidence presented by other studies has also revealed a large genetic variation in g_s of rose (Carvalho et al., 2015b, 2016; Fanourakis et al., 2013, 2016b, 2020b). The findings of this study together with those of other studies might be taken to indicate that progress in breeding programs for improving this trait may be readily made if selection for low g_s could be applied, without the necessity to resort to wild germplasm. Still, it is highly likely that much greater variation in g_s could be found with more extensive surveys of germplasm (within and outside) of commercial breeding programs.

Mechanisms resulting in concurrent reduced g_s may lead to net reductions in growth and yield at least in some environments, through its negative effect on carbon dioxide intake (Jackson et al., 2016). Thus, prolonged selection pressure for low g_s alone may eventually hamper plant growth and biomass. In the experiments reported here or earlier studies (Giday et al., 2013a, 2015), g_s was not correlated with plant biomass.

4.2. *Extended g_s prediction model*

At lower RH levels, prediction quality of the BWB-model decreased. An earlier reported model artefact (e.g. Amitrano et al., 2020) lies in the fact that the steady-state BWB-g_s model has been characterised as a correlation rather than a mechanistic equation (Gutschick & Simonneau, 2002) and is not designed for all RH conditions. The simplicity of this model, however, increased its strength in suitability as sub-models in larger model systems (Körner & Holst, 2017).

Two cultivars with a consistently large difference in g_s and ET_c ['Flirt' (low values) vs 'Alaska' (high values), respectively] across experiments of this and earlier (Giday et al., 2013b, 2015) studies were selected out of a group of six pot rose cultivars. By using these two cultivars, we have first extended the existing g_s prediction model (BWB-model) for rose by incorporating A_p or D_s as QTL-related input variables and then focussed on the extension with the same traits on the low transpiring cultivar 'Flirt' with the more complex extension of the BWB-model, i.e. the BWB-Liu-model (Liu et al., 2009). The extended model with cultivar specific parameters, as presented here, is an improvement to the BWB-Liu-model in terms of prediction quality. The BWB-Liu model without further extensions has shown

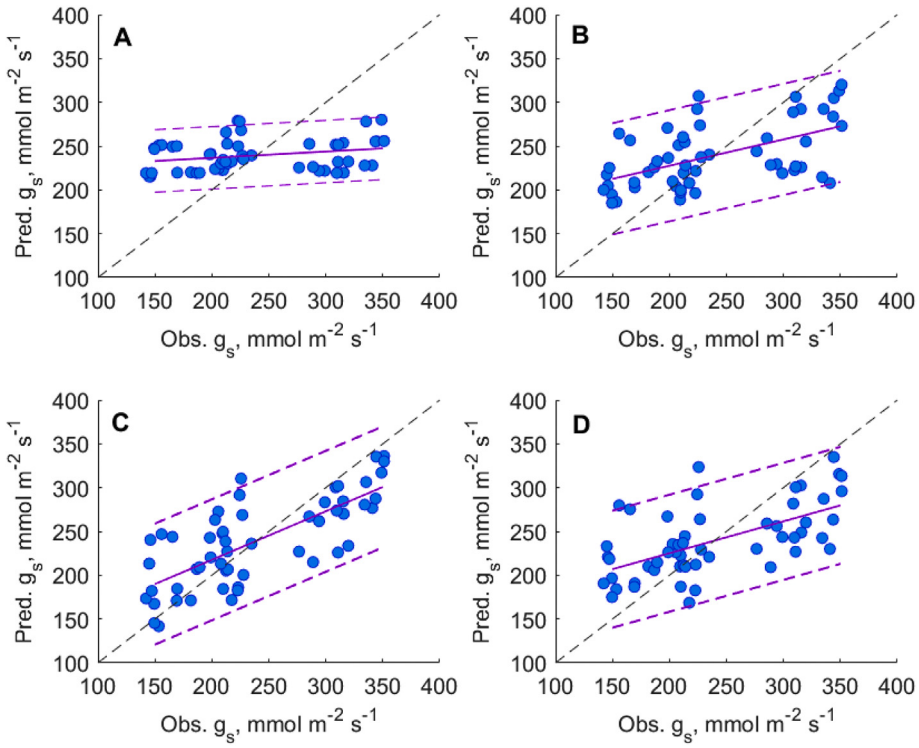

Fig. 13 – Observed versus predicted stomatal conductance (g_s) by using different models in 'Flirt' in Exp. 6: A, BWB model ($R^2 = 0.12$); B, BWB-Liu model ($R^2 = 0.31$); C, modified BWB-Liu model with individual stomatal pore area, A_p, ($R^2 = 0.52$); D, modified BWB-Liu model with stomatal density, D_s, ($R^2 = 0.59$).

improvements of model fit, which is in agreement with earlier findings (e.g. Wei et al., 2018). The extended model introduces only one additional variable, beyond those required in the existing g_s prediction model (BWB-Liu-model) (Liu et al., 2009), remarkably further improving g_s prediction quality over a range of RH levels.

The ability of the extended model was examined by comparing the estimated values with experimental measurements (Fig. 13). In contrast to substantial deviations of the existing models (BWB-model and BWB-Liu-model) (Ball et al., 1987; Liu et al., 2009), the extended version quoted here accurately reproduced the variation of g_s within one cultivar. This improvement of the extended model is achieved with the accommodation of the stomatal feature A_p or D_s. These two (cultivar-dependent) features were added separately as dynamic parameters, i.e. changing with time. However, while A_p is a rapidly changing parameter, D_s only changes in the long-term and is determined constant for each leaf. The choice of extension will have important implications for model application in climate regulation of stomata in general (Ball et al., 1987) and its use in modelling water use efficiency of crops in relation to water availability and irrigation (Liu et al., 2009). With the extended BWB-Liu model, ET_c errors associated with g_s estimations were reduced in comparison to previous models (Fig. 13). While this is at the cost of only a slight increase of model complexity, the additional input variables to the model as the fast dynamics of A_p and Ψ or the long-term changing D_s could be an obstacle in commercial usage in decision support systems (DSS) or a climate controller.

We have shown that environmental variables influence the stomatal traits and those influences are variety specific. Thus, for practical application in DSS or model-based climate control, the dynamics of these traits need to be incorporated, i.e. the dynamic model of stomatal aperture. As the stimulation of stomatal responsiveness is proportional to the increase in ABA (Giday, 2014), setting it as a major determinant of stomatal regulation (Carvalho, Torre, et al., 2015), ABA-based deterministic models (i.e. without measurements) would undoubtedly improve both model prediction quality and usability. For the BWB-Liu model application, a model or sensor for substrate Ψ is an additional need.

It is worth noting that rose is a hypostomatous species (Fanourakis et al., 2015, 2019b). Next to dynamic modelling of A_p and D_s, further investigations are thus needed on how D_s is parameterised in species with uneven distribution of stomata on the two sides of the leaf. The stomatal aperture (employed to compute A_p) is dynamic and dependent on the daily climate fluctuations, and may therefore be complicated to parameterise under some growth conditions (Fanourakis et al., 2020). Contrary to this, D_s is only affected by the long-term climate pattern (during plant growth), and with the current development of digital microscope scanners is fairly simple to be quantified (Song et al., 2020). Although extensions with A_p result in better improvements of fitting quality, the BWB-Liu model extended by D_s may have wider applications in modelling involving g_s both in protected cultivation and open field agriculture. However, for the time being, we have chosen to use the BWB-model, which has a reasonably good prediction

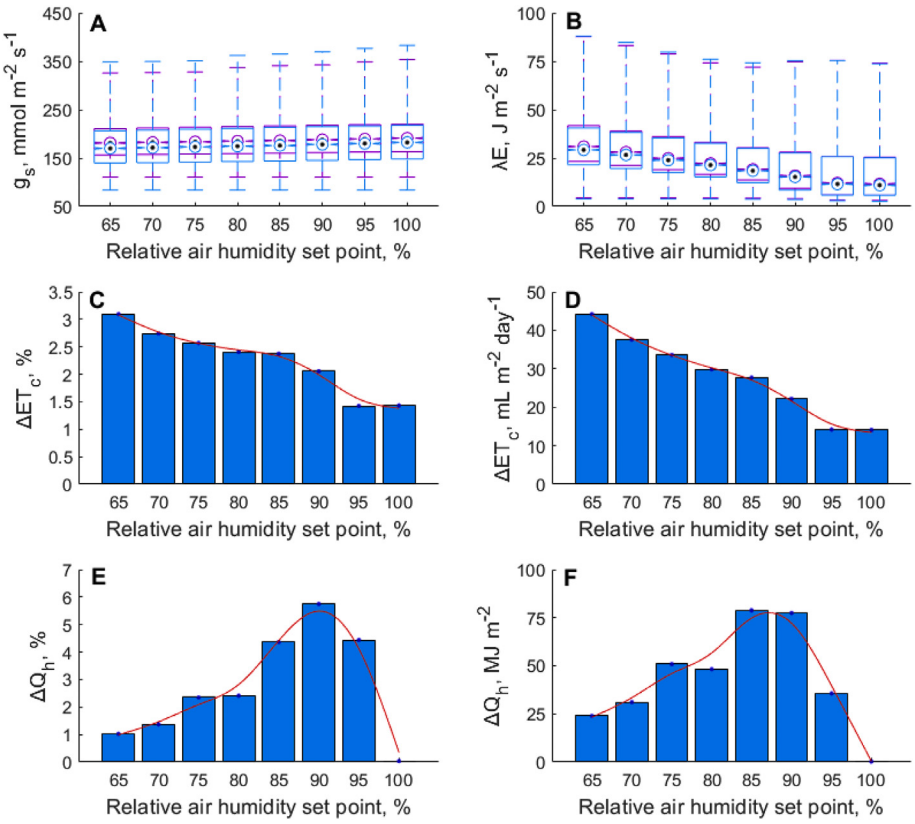

Fig. 14 – Daytime [inside light radiation >10 W m^{-2}] stomatal conductance (g_s; A), and latent heat of evaporation (λE; B) of two most contrasting pot rose cultivars ('Alaska', magenta; 'Flirt', cyan), as well as their relative and absolute difference in crop evapotranspiration (ΔET$_c$; C and D), and heat energy consumption (ΔQ$_h$; E and F). Simulations included 8 relative air humidity set point scenarios (65–100% in steps of 5%), using the same greenhouse and planting set-up with hourly climate data from the Danish Design Reference Year (Wang et al., 2013). (For interpretation of the references to colour in this figure legend, the reader is referred to the Web version of this article.)

quality at the higher RH levels that prevail in protected cultivation of ornamentals, to show the effect of cultivar selection on greenhouse energy household.

4.3. *Energy saving with cultivar selection*

Adjusted RH-based climate control can strongly reduce energy demand in greenhouses (Körner & Challa, 2004), while implementing RH-related algorithms in a greenhouse climate controller especially in modern highly insulated greenhouses is the preferred choice (Körner & Van Straten, 2008). In our investigations, we created the basis for a cultivar specific model-based climate control system. Simulations have shown that the system is robust for estimating ET$_c$ over diverse pot rose cultivars and environmental conditions (Fig. 11–13). The satisfactory agreement between actual data and estimated values indicated the strengths of the extended model as a framework and a reference for validating other approaches of calculating g_s. However, we have also shown that model extension would strongly improve prediction of g_s. In our validation study, the effect of a low prediction quality of the basic BWB-model was not evident, probably due to the higher RH levels during cultivation, as the low prediction quality comes mainly from situations at low humidity (<60%). For conditions with low RH, a model improvement needs to be done. A possible starting point is incorporating dynamic stomatal behaviour, as suggested by Vialet-Chabrand et al. (2013). While these dynamics were introduced with mathematical measures, to understand and apply future dynamic g_s models in a wide range of varieties and crops, deterministic approaches as discussed above with deterministic modelling of the role of ABA in g_s regulation would be preferable. However, for any type of model for energy saving and crop-based climate control, crop and cultivar specific parameterisation of the underlying models is of utmost importance.

5. Conclusions

The RH control can currently account for over 20% of greenhouse energy demand. Our aim was to reduce this share by considering cultivar g_s differences in estimating ET$_c$. Large differences in ET$_c$ (>20%) were noted among pot rose cultivars, which together with environmentally-induced variation resulted to a wide ET$_c$ range. This range was used to adapt and extend the BWB-Liu model, parameterise, calibrate and validate the

underlying parameters and finally implement it in a greenhouse simulator. The modified g_s-model version (considering D_s) largely improved g_s estimation (R^2 of 0.59 vs 0.31) at RHs lower than 60%. A very good agreement between simulated and measured ET_c was achieved. Depending on the RH set point, selecting low-transpiring cultivars may save between 2.5 and 5.75% of energy demand on annual basis. Incorporating the presented cultivar specific model in decision support tools and climate control would enable model-based controllers to adjust climate more efficiently (with real-time DSS), and create ground for planning tools in greenhouse construction (in association with greenhouse planning tools such as Virtual Greenhouse).

Authors' contribution

MCRH, DHL, and BH performed the experimental work. MCRH and OK created the stomatal conductance model approach. OK carried out the simulation studies, data analysis and interpretation. DF assisted the data interpretation, and together with OK wrote the manuscript. GT and CD participated in data interpretation, and provided valuable insights. COO and ER designed and supervised the study. All authors have read and agreed to the published version of the manuscript.

Declaration of competing interest

The authors declare that they have no known competing financial interests or personal relationships that could have appeared to influence the work reported in this paper.

Acknowledgements

The work was supported by funding from the project RedHum, nr. 34009-14-0781 from Green Development and Demonstration Programme. We thank the rose producer Rosa Danica for providing the plants for all experiments. We are indebted to René Hvidberg Petersen and Lene Klem at University of Copenhagen and Ruth Nielsen, Kai Ole Dideriksen and Helle Kjærsgaard Sørensen at Aarhus University for their contributions, continued diligence, and dedication to their craft as growers and technicians. The valuable comments of the editor and three anonymous reviewers are greatly acknowledged.

REFERENCES

Aaslyng, J. M., Lund, J. B., Ehler, N., & Rosenqvist, E. (2003). Intelligrow: A greenhouse component-based climate system. *Environmental Modelling & Software, 18*, 657–666.

Amitrano, C., Chirico, G. B., De Pascale, S., Rouphael, Y., & De Micco, V. (2020). Crop management in controlled environment agriculture (CEA) systems using predictive mathematical models. *Sensors, 20*, 3110.

Amitrano, C., Rouphael, Y., De Pascale, S., & De Micco, V. (2021). Modulating vapor pressure deficit in the plant microenvironment may enhance the bioactive value of lettuce. *Horticulturae, 7*(2), 32.

Ball, J. T., Woodrow, I. E., & Berry, J. A. (1987). A model predicting stomatal conductance and its contribution to the control of photosynthesis under different environmental conditions. In J. Biggins (Ed.), *Progress in photosynthesis research* (pp. 221–224). Dordrecht, The Netherlands: Martinus Nijhoff.

Bot, G. P. A. (2001). Developments in indoor sustainable plant production with emphasis on energy saving. *Computers and Electronics in Agriculture, 30*, 151–165.

Carvalho, D. R. A., Fanourakis, D., Correia, M. J., Monteiro, J. A., Araújo-Alves, J. P. L., Vasconcelos, M. W., Almeida, D. P. F., Heuvelink, E., & Carvalho, S. M. P. (2016). Root-to-shoot ABA signalling does not contribute to genotypic variation in stomatal functioning induced by high relative air humidity. *Environmental and Experimental Botany, 123*, 13–21.

Carvalho, D. R. A., Koning-Boucoiran, C. F. S., Fanourakis, D., Vasconcelos, M. W., Carvalho, S. M. P., Heuvelink, E., Krens, F. A., & Maliepaard, C. (2015). QTL analysis for stomatal functioning in tetraploid Rosa × hybrida grown at high relative air humidity and its implications on postharvest longevity. *Molecular Breeding, 35*, 172.

Carvalho, D., Torre, S., Kraniotis, D., Almeida, D. P. F., Heuvelink, E., & Carvalho, S. M. P. (2015). Elevated air movement enhances stomatal sensitivity to abscisic acid in leaves developed at high relative air humidity. *Frontiers in Plant Science, 6*, 1–11.

Dow, G. J., Berry, J. A., & Bergmann, D. C. (2014). The physiological importance of developmental mechanisms that enforce proper stomatal spacing in Arabidopsis thaliana. *New Phytologist, 201*, 1205–1217.

Fanourakis, D., Aliniaeifard, S., Sellin, A., Giday, H., Körner, O., Rezaei Nejad, A., Delis, C., Bouranis, D., Koubouris, G., Kambourakis, E., Nikoloudakis, N., & Tsaniklidis, G. (2020). Stomatal behavior following mid- or long-term exposure to high relative air humidity: A review. *Plant Physiology and Biochemistry, 153*, 92–105.

Fanourakis, D., Bouranis, D., Giday, H., Carvalho, D. R. A., Rezaei Nejad, A., & Ottosen, C. O. (2016). Improving stomatal functioning at elevated growth air humidity: A review. *Journal of Plant Physiology, 207*, 51–60.

Fanourakis, D., Bouranis, D., Tsaniklidis, G., Rezaei Nejad, A., Ottosen, C. O., & Woltering, E. J. (2020). Genotypic and phenotypic differences in fresh weight partitioning of cut rose stems: Implications for water loss. *Acta Physiologia Plantarum, 42*, 48.

Fanourakis, D., Giday, H., Hyldgaard, B., Bouranis, D., Körner, O., & Ottosen, C. O. (2019). Low air humidity during growth promotes stomatal closure ability in potted roses (Rosa hybrida). *European Journal of Horticultural Science, 84*, 245–252.

Fanourakis, D., Giday, H., Li, T., Kambourakis, E., Ligoxigakis, E. K., Papadimitriou, M., Strataridaki, A., Bouranis, D., Fiorani, F., Heuvelink, E., & Ottosen, C. O. (2016). Antitranspirant compounds alleviate the mild-desiccation-induced reduction of vase life in cut roses. *Postharvest Biology and Technology, 117*, 110–117.

Fanourakis, D., Giday, H., Milla, R., Pieruschka, R., Kjaer, K. H., Bolger, M., Vasilevski, A., Nunes-Nesi, A., Fiorani, F., & Ottosen, C. O. (2014). Pore size regulates operating stomatal conductance, while stomatal densities drive the partitioning of conductance between leaf sides. *Annals of Botany, 115*, 555–565.

Fanourakis, D., Heuvelink, E., & Carvalho, S. M. P. (2013). A comprehensive analysis of the physiological and anatomical components involved in higher water loss rates after leaf development at high humidity. *Journal of Plant Physiology, 170*, 890–898.

Fanourakis, D., Heuvelink, E., & Carvalho, S. M. P. (2015). Spatial heterogeneity in stomatal features during leaf elongation: An analysis using Rosa hybrida. *Functional Plant Biology, 42*, 737–745.

Fanourakis, D., Hyldgaard, B., Giday, H., Aulik, I., Bouranis, D., Körner, O., & Ottosen, C. O. (2019). Stomatal anatomy and closing ability is affected by supplementary light intensity in rose (Rosa hybrida L.). *Horticultural Science – Prague, 46*, 81–89.

Fanourakis, D., Hyldgaard, B., Giday, H., Bouranis, D., Körner, O., Nielsen, K. L., & Ottosen, C. O. (2017). Differential effects of elevated air humidity on stomatal closing ability of Kalanchoë blossfeldiana among the C3 and CAM states. *Environmental and Experimental Botany, 143*, 115–124.

Fanourakis, D., Kazakos, P., & Nektarios, P. A. (2021). Allometric individual leaf area estimation in chrysanthemum. *Agronomy, 11*, 795.

Fanourakis, D., Nikoloudakis, N., Pappi, P., Markakis, E., Doupis, G., Charova, S., Delis, C., & Tsaniklidis, G. (2020). The role of proteases in determining stomatal development and tuning pore aperture: A review. *Plants, 9*, 340.

Fanourakis, D., Tapia, A., Carvalho, S. M. P., & Heuvelink, E. (2008). Cultivar differences in the stomatal characteristics of cut roses grown at high relative humidity. *Acta Horticulturae, 847*, 251–258.

Farquhar, G. D., & Von Caemmerer, S. (1982). Modelling of photosynthetic response to environmental conditions. In O. L. Lange, P. S. Nobel, C. B. Osmond, & H. Ziegler (Eds.), *Water relations and carbon assimilation. Encyclopedia of plant physiology. New-series. Physiological plant ecology II* (pp. 549–587). Berlin, Germany: Springer-Verlag.

Farquhar, G. D., Von Caemmerer, S., & Berry, J. A. (1980). A biochemical model of photosynthetic CO2 assimilation in leaves of C3 species. *Planta, 149*, 78–90.

Franks, P. J., Drake, P. L., & Beerling, D. J. (2009). Plasticity in maximum stomatal conductance constrained by negative correlation between stomatal size and density: An analysis using Eucalyptus globulus. *Plant, Cell and Environment, 32*, 1737–1748.

Gelder, A.d., Dieleman, J. A., Bot, G. P. A., & Marcelis, L. F. M. (2012). An overview of climate and crop yield in closed greenhouses. *Journal of Horticultural Science and Biotechnology, 87*, 193–202.

Giday, H. (2014). *On the role of abscisic acid in the regulation of phenotypic and genetc variation in stomatal closing ability*. PhD Thesis (p. 129). Denmark, Aarhus: Aarhus University.

Giday, H., Fanourakis, D., Kjaer, K. H., Fomsgaard, I. S., & Ottosen, C. O. (2013). Foliar abscisic acid content underlies genotypic variation in stomatal responsiveness after growth at high relative air humidity. *Annals of Botany, 112*, 1857–1867.

Giday, H., Fanourakis, D., Kjaer, K. H., Fomsgaard, I. S., & Ottosen, C. O. (2014). Threshold response of stomatal closing ability to leaf abscisic acid concentration during growth. *Journal of Experimental Botany, 65*, 4361–4370.

Giday, H., Kjaer, K. H., Fanourakis, D., & Ottosen, C. O. (2013). Smaller stomata require less severe leaf drying to close: A case study in Rosa hydrida. *Journal of Plant Physiology, 170*, 1309–1316.

Giday, H., Kjaer, K. H., Ottosen, C. O., & Fanourakis, D. (2015). Cultivar differences in plant transpiration rate at high relative air humidity are not related to genotypic variation in stomatal responsiveness. *Acta Horticulturae, 1064*, 99–106.

Gijzen, H. (1994). *Ontwikkeling van een simulatiemodel voor transpiratie en wateropname en van een integral gewasmodel. (Development of a simulation model for transpiration and water uptake and an integral crop model)* (Vol. 18). Wageningen, The Netherlands: AB-DLO.

Goddek, S., & Körner, O. (2019). A fully integrated simulation model of multi-loop aquaponics: A case study for system sizing in different environments. *Agricultural Systems, 171*, 143–154.

Gutschick, V., & Simonneau, T. (2002). Modelling stomatal conductance of field-grown sunflower under varying soil water content and leaf environment: Comparison of three models of stomatal response to leaf environment and coupling with an abscisic acid-based model of stomatal response to soil drying. *Plant, Cell and Environment, 25*, 1423–1434.

Hassanvand, F., Nejad, R. A., & Fanourakis, D. (2019). Morphological and physiological components mediating the silicon-induced enhancement of geranium essential oil yield under saline conditions. *Industrial Crops and Products, 134*, 19–25.

Ho, L. C., Belda, R., Brown, M., Andrews, J., & Adams, P. (1993). Uptake and transport of calcium and the possible causes of blossom-end rot in tomato. *Journal of Experimental Botany, 44*, 509–518.

Islam, M. N., Körner, O., Pedersen, J. S., Sørensen, J. N., & Edelenbos, M. (2019). Analyzing quality and modelling weight loss of onions during drying and storage. *Computers and Electronics in Agriculture, 164*, 104865.

Jackson, P., Basnayake, J., Inman-Bamber, G., Lakshmanan, P., Natarajan, S., & Stokes, C. (2016). Genetic variation in transpiration efficiency and relationships between whole plant and leaf gas exchange measurements in Saccharum spp. and related germplasm. *Journal of Experimental Botany, 67*, 861–871.

Janka, E., Körner, O., Rosenqvist, E., & Ottosen, C. O. (2016). A coupled model of leaf photosynthesis, stomatal conductance, and leaf energy balance for chrysanthemum (Dendranthema grandiflora). *Computer and Electronics in Agriculture, 123*, 264–274.

Kim, S. H., & Lieth, J. H. (2003). A coupled model of photosynthesis, stomatal conductance and transpiration for a rose leaf (Rosa hybrida L.). *Annals of Botany, 91*, 771–781.

Kohtaro, I., & Olajumoke, O. (2020). A new indicator of leaf stomatal conductance based on thermal imaging for field grown cowpea. *Plant Production Science, 23*, 136–147.

Körner, O. (2004). Evaluation of crop photosynthesis models for dynamic climate control. *Acta Horticulturae, 654*, 295–302.

Körner, O., Aaslyng, J. M., Andreassen, A. U., & Holst, N. (2007). Microclimate prediction for dynamic greenhouse climate control. *HortScience, 42*, 272–279.

Körner, O., Bakker, M. J., & Heuvelink, E. (2004). Daily temperature integration: A simulation study to quantify energy consumption. *Biosystems Engineering, 87*, 333–343.

Körner, O., & Challa, H. (2003a). Design for an improved temperature integration concept in greenhouse cultivation. *Computers and Electronics in Agriculture, 39*, 39–59.

Körner, O., & Challa, H. (2003b). Process-based humidity control regime for greenhouse crops. *Computers and Electronics in Agriculture, 39*, 173–192.

Körner, O., & Challa, H. (2004). Temperature integration and process-based humidity control in chrysanthemum. *Computers and Electronics in Agriculture, 43*, 1–21.

Körner, O., & Hansen, J. B. (2012). An on-line tool for optimising greenhouse crop production. *Acta Horticulturae, 957*, 147–154.

Körner, O., & Holst, N. (2017). An open source greenhouse modelling platform. *Acta Horticulturae, 1154*, 241–248.

Körner, O., & Van Straten, G. (2008). Decision support for dynamic greenhouse climate control strategies. *Computers and Electronics in Agriculture, 60*, 18–30.

Koubouris, G., Bouranis, D., Vogiatzis, E., Rezaei Nejad, A., Giday, H., Tsaniklidis, G., Ligoxigakis, E. K., Blazakis, K., Kalaitzis, P., & Fanourakis, D. (2018). Leaf area estimation by considering leaf dimensions in olive tree. *Scientia Horticulturae, 240*, 440–445.

Liu, F., Andersen, M. N., & Jensen, C. R. (2009). Capability of the 'Ball-Berry' model for predicting stomatal conductance and water use efficiency of potato leaves under different irrigation regimes. *Scientia Horticulturae, 122*, 346–354.

Medlyn, B. E., Duursma, R. A., Eamus, D., Ellsworth, D. S., Prentice, C., Bartons, C. G., Crous, K. Y., De Angelis, P., Freeman, M., & Wingate, L. (2011). Reconciling the optimal and empirical approaches to modelling stomatal conductance. *Global Change Biology, 17*, 2134–2144.

Merilo, E., Jõesaar, I., Brosché, M., & Kollist, H. (2014). To open or to close: Species-specific stomatal responses to simultaneously applied opposing environmental factors. *New Phytologist, 202*, 499–508.

Opdam, J. J. G., Schoonderbeek, G. G., Heller, E. M. B., & De Gelder, A. (2005). Closed greenhouse: A starting point for sustainable entrepreneurship in horticulture. *Acta Horticuturae, 691*, 517–524.

Seif, M., Aliniaeifard, S., Arab, M., Mehrjerdi, M. Z., Shomali, A., Fanourakis, D., Li, T., & Woltering, E. (2021). Monochromatic red light during plant growth decreases the size and improves the functionality of stomata in chrysanthemum. *Functional Plant Biology, 48*, 515–528.

Song, W., Li, J., Li, K., Chen, J., & Huang, J. (2020). An automatic method for stomatal pore detection and measurement in microscope images of plant keaf based on a convolutional neural network model. *Forests, 11*, 954.

Sørensen, H. K., Fanourakis, D., Tsaniklidis, G., Bouranis, D., Rezaei Nejad, A., & Ottosen, C. O. (2020). Using artificial lighting based on electricity price without a negative impact on growth, visual quality or stomatal closing response in Passiflora. *Scientia Horticulturae, 267*, 109354.

Thornley, J. H. M. (1976). *Mathematical models in plant physiology*. London, UK: Academic Press (Inc.).

Vadiee, A., & Martin, V. (2012). Energy management in horticultural applications through the closed greenhouse concept, state of the art. *Renewable and Sustainable Energy Reviews, 16*, 5087–5100.

Van Genuchten, M. T. (1980). A closed form equation for predicting hydraulic conductivity of unsaturated soils. *Soil Society of America Journal, 44*, 892–898.

Van Kraalingen, D. W. G., & Rappoldt, C. (1989). *Subprograms in simulation models. 18*. Wageningen, The Netherlands: CABO.

Vanthoor, B. (2011). *A model-based greenhouse design method*. Wageningen, The Netherlands: Wageningen University.

Vialet-Chabrand, S., Dreyer, E., & Brendel, O. (2013). Performance of a new dynamic model for predicting diurnal time courses of stomatal conductance at the leaf level. *Plant, Cell and Environment, 36*, 1529–1546.

Wang, P. G., Scharling, M., Pagh Nielsen, K., Kern-Hansen, C., & Wittchen, K. B. (2013). *Danish design reference year: Reference climate dataset for technical dimensioning in building, construction and other sectors*. Danmarks Meteorologiske Institut.

Wei, Z., Du, T., Li, X., Fang, L., & Liu, F. (2018). Simulation of stomatal conductance and water use efficiency of tomato leaves exposed to different irrigation regimes and air CO2 concentrations by a modified "Ball-Berry" model. *Frontiers in Plant Science, 9*.

Zhang, D., Du, Q., Zhang, Z., Jiao, X., Song, X., & Li, J. (2017). Vapour pressure deficit control in relation to water transport and water productivity in greenhouse tomato production during summer. *Scientific Reports, 7*, 43461.